UPPSALA
UNIVERSITET

UPTEC X 20005
Examensarbete 30 hp
Juni 2020

Implementation of the mille-feuille nanofilter paper in the virus removal filtration of IgY purified from chicken egg yolk

Michelle Dahlman

UPPSALA
UNIVERSITET

Teknisk- naturvetenskaplig fakultet
UTH-enheten

Besöksadress:
Ångströmlaboratoriet
Lägerhyddsvägen 1
Hus 4, Plan 0

Postadress:
Box 536
751 21 Uppsala

Telefon:
018 – 471 30 03

Telefax:
018 – 471 30 00

Hemsida:
http://www.teknat.uu.se/student

Abstract

Implementation of the mille-feuille nanofilter paper in the virus removal filtration of IgY purified from chicken egg yolk

Michelle Dahlman

The purpose of this thesis was to test the mille-feuille nanofilter paper for a virus removal filtration from a potential protein-based nutraceutical. Therefore, chicken IgY was purified from egg yolk, with PEG precipitation for crude fractionation followed by thiophilic adsorption chromatography. The biuret total protein assay was done for quantitative analysis, and for qualitative analyses, sodium dodecyl sulphate-polyacrylamide gel electrophoresis, dynamic light scattering and size exclusion-high performance liquid chromatography were performed. The protein characterization results revealed that the final preparation of IgY was a complex mixture of proteins and aggregates.

Two variants of the mille-feuille filter paper were produced for the two-step nanofiltration: 11 µm pre-filters to remove aggregates and other high molecular weight impurities, as well as dedicated 31 µm virus removal filters. The thickness, basis weight and hydraulic flux of the produced filters were measured for quality control, and the pore size distributions of the filters were estimated with the use of cryoporometry by differential scanning calorimetry and the BJH method derived from nitrogen gas sorption isotherms.

Finally, the IgY preparation was spiked with the model virus ΦX174 and tested for virus removal with the mille feuille filter paper, which resulted in an LRV over 5 as determined with the plaque forming units assay. Flux measurements as well as following pre-filtrate and filtrate characterizations with dynamic light scattering revealed that the pre-filtration had a critical impact on the quality of the final product. The final filtrate was gone through tandem mass spectrometry, upon which IgY and several other egg yolk proteins were identified. The results of this thesis show that the mille-feuille nanofilter paper has a high potential for virus removal of nutraceuticals.

Keywords: Virus removal filtration, Mille-feuille filter paper, Chicken IgY, Protein purification

Handledare: Albert Mihranyan
Ämnesgranskare: Gunnar Johansson
Examinator: Erik Holmqvist
ISSN: 1401-2138, UPTEC X 20005

Implementation of the mille-feuille nanofilter paper in the virus removal filtration of IgY purified from chicken egg yolk

Michelle Dahlman

Populärvetenskaplig sammanfattning

Äggulan från höns är rik på bioaktiva proteiner och peptider, däribland immunoglobulin Y. Immunoglobulin Y är fåglars motsvarighet till däggdjurens immunoglobulin G. Immunglobuliners uppgift i immunförsvaret är att oskadliggöra främmande antigener, och dess unika målsökande egenskap kan vidare användas i nutraceuticals där de visar särskild lämplighet för användandet inom passiv immunisering för att motverka humana virus i mag- och tarmkanalen.

Inom produktionen av alla proteinbaserade läkemedel och nutraceuticals finns det alltid en risk för viruskontaminering. Dels kan råmaterialet innehålla patogener farliga för människan eller också kan sådana introduceras under tillverkningsprocessen. Det är därför viktigt att införa virusborttagningsmetoder i produktionen som ser till att biosäkerheten för den slutgiltiga produkten säkerställs och är helt fri från patogener. Det finns olika metoder för virusborttagning som alla har sina fördelar och begränsningar. Somliga proteiners bioaktivitet, däribland immunoglobuliner, kan dock påverkas av flertalet av dessa virusborttagningsmetoder. Nanofiltrering är en attraktiv metod för virusborttagning via storleksseparation då den kan avlägsna de allra flesta virus utan att påverka proteinets funktion. Deras höga kostnad är dock en stor nackdel, varpå det finns en stor efterfrågan på en ny typ av nanofilter som kan kombinera hög prestanda med kostnadseffektivitet.

Mihranyans grupp på Uppsala universitet har utvecklat ett nanofilter, kallat mille-feuille filter, producerat helt från cellulosa utvunnen från grönalgen *Cladophora* och har stora möjligheter att möta denna efterfrågan. Filtret har visat hög potential inom virusborttagning inom en rad applikationer, men har ännu ej testats inom tillverkningen av nutraceuticals. I detta examensarbete har därför immunoglobulin Y renats från äggula för att sedan användas i ett virusborttagningstest med mille-feuille filtret. Resultaten visar att mille-feuille filtret har en hög potential för virusborttagning.

Examensarbete 30 hp
Civilingenjörsprogrammet i Molekylär bioteknik

Table of contents

List of Abbreviations

BSL	Biosafety Level
CP-DSC	Cryoporometry by Differential Scanning Calorimetry
DLS	Dynamic Light Scattering
HC	Heavy Chain
hIVIG	Human Intravenous Immunoglobulins
IEX	Ion Exchange Chromatography
IgG	Immunoglobulin G
IgY	Immunoglobulin Y
LC	Light Chain
LRV	Log_{10} Reduction Value
MS-LC	Mass Spectrometry- Liquid Chromatography
NGSP	Nitrogen Gas Sorption Porometry
SE-HPLC	Size Exclusion- High Performance Liquid Chromatography
SDS-PAGE	Sodium Dodecyl Sulphate- Polyacrylamide Gel Electrophoresis
PBS	Phosphate Buffered Saline
PFU	Plaque Forming Units
pI	Isoelectric Point
TAC	Thiophilic Adsorption Chromatography
TMP	Transmembrane Pressure

1 Introduction

Chicken IgY has been of considerable interest in several applications, including that as an active agent in nutraceuticals. IgY has shown high potential in the application of orally administered antibodies in passive immunisation as an alternative treatment to vaccine and antibiotics against viral and bacterial infections in the gastrointestinal tract (Carlander et *al.* 2000). Sarker et *al*. (2001) showed that oral administration of human rotavirus-specific IgY extracted from hens to children with rotavirus diarrhoea exhibited significant protective effect. Horie et *al*. (2004) demonstrated the abolishment of *Helicobacter pylori* infection in humans through oral administration of neutralizing IgY antibodies in drinking yoghurt.

In the development of all protein-based pharmaceuticals and nutraceuticals there is a risk of viral contamination. In order to ensure the biosafety of the final product, a range of virus clearance steps can be implemented in the manufacturing process. For immunoglobulin, commonly used inactivation methods like irradiation (UV-C, γ-radiation) and heat treatment (high temperature short time (HTST)) are incompatible due to possible denaturation of proteins (Grieb, T. et *al.* 2002). Therefore, there is a need for novel methods for viral clearance that ensure both the biosafety and the bioactivity of protein nutraceuticals.

The mille-feuille filter paper developed by Mihranyan's group at Uppsala University show high potential to meet both needs. The nanofilter is the first non-woven size-exclusion virus removal filter produced entirely out of the cellulose from *Cladophora* green algae (Metreveli et *al.* 2014; Gustafsson et *al.* 2016). The filter has shown high potential in the virus removal application such as downstream and upstream bioprocessing as well as drinking water purification. However, its application in the processing of nutraceuticals is yet to be tested. Therefore, in this thesis, chicken IgY will be isolated and purified from egg yolk and subsequently gone through a virus removal filtration with the the mille-feuille filter paper.

2 Background

2.1 Chicken egg proteomics

Chicken eggs are a natural food source for humans, and the yolk is rich in bioactive proteins and peptides that can further be used as pharmaceutical or nutraceutical agents (Mine & Kovacs-Nolan 2006). The yolk is a very complex assembly of lipids and proteins where proteins exist as either free proteins or as apoproteins, i.e. proteins that form assemblies with lipids into low-and high-density lipoproteins which are the main constituents of yolk. The yolk can further be divided into a water-soluble plasma phase and a granola fraction. The plasma main constituents are low-density lipoproteins and three groups of livetin proteins: α-livetin (serum albumin), β-livetin, and γ-livetin (IgY). The granular phase contains α- and β-lipovitellins, phosvitin and low-and high-density lipoproteins. Overall, the proteins with highest abundance in egg yolk have been identified as IgY, serum albumin, cleavage products of vitellogenin, apovitellogenins, and ovalbumin (Mann & Mann 2008).

2.2 Comparisons of chicken IgY and mammalian IgG

Chicken IgY is the major serum antibody in hens and consists of two heavy chains and two light chains. Instead of the typical Ig hinge region located between the antigen binding region (Fab) and constant region (Fc), IgY possesses an extra pair of heavy chain constant domains resulting in a less flexible protein structure (Carlander et *al.* 1999). As the Fc region is the most hydrophobic part of an Ig, the extra pair of constant domains on the heavy chain makes IgY more hydrophobic than mammalian IgG. The isoelectric point (pI) of chicken IgY reportedly is lower (5.6-7.5) than that of mammalian IgG (6.9-9.0) (Li et *al.* 2002). Also, the molecular weight of IgY is higher (180 kDa) than that of mammalian IgG (150 kDa) (Carlander et *al.* 1999). There are several other important differences from mammalian IgG. For example, IgY does not bind to human Fc-receptors, complement factors or protein A and G, which reduces the risk of non-specific immune responses but complicates the purification process as the later are effective and commonly used ligands in affinity chromatography in purification of Igs (Larsson et *al.* 1998).

There are many advantages to use chicken IgY in applications where mammalian IgG and other antibodies are currently used. Eggs are cheap and readily available, and the maternal transfer of IgY from hen serum to egg yolk enables a non-invasive and easier way of extraction than that of mammalian antibodies (Carlander et *al.* 2000; Jensenius et *al.* 1981). Furthermore, the IgY productivity in laying hens is almost 18 times greater than that of IgG in rabbits (Schade et *al.* 2001), and the phylogenetic distance between mammalians and avians results in a higher titer of mammalian antigen-specific antibodies produced in avians than in mammalians (Carlander et *al.* 1999).

2.3 Viral clearance methods

Chicken eggs may already be contaminated with potential human pathogens like *Salmonellas*, *Campylobacter* spp. and *Listeria* spp. which are the most frequent sources of food-borne disease outbreaks (Jones et *al.* 2012). Avian viruses are also of concern. Hence, in the following extraction and purification of egg-derived proteins for their use in nutraceuticals, there will be a continuous risk of viral contamination in the manufacturing environment. Therefore, it is essential, as in the manufacturing of all protein-based pharmaceutics, to implement virus clearance steps in the process in order to ensure the biosafety of the final product. Virus clearance methods are classified as either inactivation or removal methods. Among inactivation methods, low pH, solvent/detergent, UV-C irradiation, γ-irradiation and heat treatments, e.g. pasteurization, are commonly used methods, whereas nanofiltration can be used for virus removal (Shukla & Aranha 2015; Boschetti et *al.* 2005). Table 1 shows an overview of common clearance methods in protein bioprocessing, with target virus types, limitations and advantages. Overall, the inactivation methods are based on the protein having higher resistance to inactivation than the viruses, which is not always the case. Non-enveloped viruses are more challenging to eliminate as the lack of lipid coat has made them naturally more resistant to harsh conditions, and therefore show high resistance to some inactivation methods, e.g. to low pH, solvent/detergent and heat treatments (Gröner et al. 2018). Moreover, heat treatments, e.g. pasteurization, and irradiation methods are incompatible with Igs and result in their denaturation and loss of their bioactivity. (Godden et *al.* 2006; Grieb et *al.* 2002)

Table 1. Overview of common viral clearance methods used in bioprocessing with target viruses, limitations and advantages. Adapted from Boschetti et *al.* 2005.

Viral clearance method	Effective against	Limitations	Advantages
Low pH	Enveloped viruses	• Not compatible with proteins sensitive to low pH (e.g. Igs) • Limited inactivation of non-enveloped viruses	Compatible with low pH mAb processes
γ-irradiation	Many viruses with different effectiveness	• Proteins may absorb radiation and denature and/or denature due to free radicals and reactive oxygen species generated during radiation	Effective against a wide range of viruses
UV-C irradiation	Many viruses with different effectiveness	• Does not inactivate all viruses, e.g. retroviruses • Proteins may absorb radiation and denature and/or denature due to free radicals and reactive oxygen species generated during radiation	Effective against a wide range of viruses
Solvent/detergent	Enveloped viruses	• Does not inactivate non-enveloped viruses • The solvent/detergent requires removal	• No protein denaturation • High protein recovery

Heat treatments (e.g. HTST)	Enveloped and many nonenveloped viruses	• Can denature certain proteins • Does not inactivate parvovirus B19 • Eventual stabilizers may require removal	• Simple process • Effective against a wide range of viruses
Nanofiltration	All viruses, size-dependent	• Very expensive • Membrane fouling	• Does not interfere with protein bioactivity • High protein recovery • Effective against a wide range of viruses

Nanofiltration is a robust method for virus removal that utilizes the size difference to separate viruses from protein solutions (Cipriano et *al.* 2012; Buchacher & Iberer 2006). Particles featured with a larger size than the size of the filter pores will be captured by the filter. Unlike the inactivation methods, nanofiltration is more attractive because it physically removes undesired particles, including the most resistant non-enveloped viruses and does not interfere with the bioactivity of the protein of interest. A limitation of nanofiltration is that the flux typically decreases during operation with fluids, due to fouling of the membranes. The fouling can be due to many reasons, e.g. accumulation of high molecular weight aggregates, but can be significantly reduced by implementing a prefiltration step (Kent et *al.* 2017). Furthermore, most currently available filters on market are ceramic membranes or made from synthetic polymers and are very expensive, partly due to their complicated production and their single use, which consequently marks the price of the final product (Buchacher & Iberer 2006). Therefore, there is an urge for a more cost-efficient high-performing nanofilter to reduce the high production cost of protein-based pharmaceutics and nutraceuticals.

The mille-feuille filter paper developed by Mihranyan's group at Uppsala University is a novel nanofilter made entirely from cellulose nanofibers derived from *Cladophora* green algae (Metreveli et *al*. 2014). The filter pores arise due to voids between randomly aligned cellulose nanofibers. The work done by Mihranyan's group enabled tailoring the pore size of the nanofilter to successfully separate proteins from both small-and large-size viruses based on the size exclusion principle. The mille-feuille filter has shown high performance in several virus removal filtrations, including the removal of swine influenza A virus (Metreveli et *al*. 2014), xenotropic murine leukemia virus (xMuLV) (Asper et *al.* 2015), and even the worst-case model minute virus of mice (MVM) (Gustafsson et *al.* 2016). Recently, the virus removal filtration of the mille-feuille filter was shown for human plasma-derived immunoglobulin G (hIVIG) spiked with ΦX174 and MS2 phages as model small-size viruses (Wu et *al.* 2019). The filter has also demonstrated high potential in water purification applications, where its ability to remove viruses and other microorganisms from water has recently been tested (Gustafsson et *al.* 2018; Manukyan et al. 2019). Apart from its high performance demonstrated in earlier mentioned studies, and with regards to currently available nanofilters, the cellulose of the mille-feuille filter makes it a more sustainable and cost-efficient product. Its feasibility in the production of nutraceuticals and functional food proteins has not yet been tested, which is the reason for this project. Various aspects of IgY isolation, purification, and virus-removal nanofiltration are discussed in more detail below.

2.4 Methods for IgY isolation and purification from chicken egg yolk

2.4.1 Crude fractionation

As earlier mentioned, chicken egg yolk is a complex mixture of water-soluble proteins, lipoproteins and lipids, and the first and most critical part of purifying IgY is to separate the protein in the plasma from the granular phase. Salt precipitation (Deignan et *al.* 2000), PEG precipitation (Schade et *al.* 2001) and ultrafiltration (Hernández-Campos et *al.* 2010) are commonly used methods for the initial fractionation of IgY. In this project, PEG precipitation was chosen for crude fractionation.

2.4.1.1 Precipitation with PEG

Polyethylene glycol (PEG) precipitation is a frequently used method for initial fractionation of IgY. PEG precipitates IgY by occupying the solvent (water) to a limit where the local concentration of IgY exceeds its solubility, somewhat similar to salting out with electrolytes (Polson et *al.* 1980). The PEG precipitation method was further developed (Polson et al. 1985) with PEG at a molecular weight of 6000, i.e. PEG-6000, to a process of three consecutive steps, starting with 3.5% of total volume of PEG to remove fatty acids, followed by 8.5% to remove lipids, and then 12% PEG to finally precipitate IgY.

2.4.2 Polishing chromatography

After the initial fractionation, IgY can be further purified using chromatography techniques. In protein purification processes in industry, two chromatography steps are often implemented to reach a highly purified final preparation of the protein in question. In this project, ion exchange chromatography and thiophilic adsorption chromatography were chosen as both methods previously have been used to purify chicken IgY.

2.4.2.1 Thiophilic adsorption chromatography (TAC)

The first process of thiophilic chromatography was developed for the isolation of Igs (Hutchens & Porath 1986), and its mechanism is not yet fully established. It has been suggested that Igs bind to an immobilized sulfone thioether ligand on the resin (Fig. 1) through a salt-promoted electron acceptor and donor mechanism of the electron free pair of a thioether and a sulfone dipole on the ligand (Porath & Belew 1987). Desorption of the proteins bound to the resin occurs when the concentration of a lyotropic salt, such as potassium sulphate, is reduced.

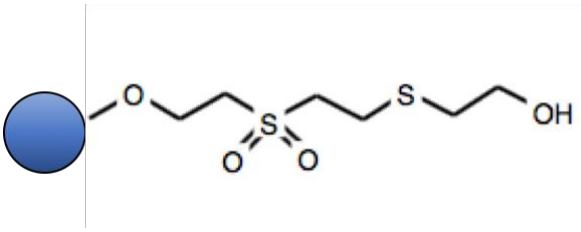

Figure 1. Schematic drawing of the molecular structure of a sulfone thioether ligand immobilized to the column resin in thiophilic affinity chromatography.

2.4.2.2 Ion exchange chromatography (IEX)

In ion exchange chromatography (IEX) separation of proteins occurs due to the charged groups of the protein surface, which is influenced by the surrounding environment (Scopes 1994). IEX can be classified as either cation exchange or anion exchange, depending on the charge of the immobilized groups to the stationary phase, which are negatively charged for cation columns and positively charged for anion columns. The charge of the protein surface depends on the pH of the surrounding environment as well as pI of the protein in question. Hence, separation of proteins can be done by actively choosing pH and salt concentration of the mobile phase that will optimize binding (bind and elute mode) or direct washout (flow-through mode) of the protein of interest. For the purification of chicken IgY, both cation exchange and anion exchange columns can be used, but the latter is mentioned more frequently in previous studies regarding IgY purification. With an anion exchange column and a buffer pH above the pI of IgY (5.6-7.5), an overall negative charge will be generated to the protein which can then bind to the column through electrostatic interactions. Other egg proteins with a pI above the pH of the buffer will instead flow through the column and can thereby be separated from IgY.

2.5 Protein characterization methods

In the purification of a specific protein, it is of crucial interest to determine the recovery and purity of the protein, the composition of the sample as well as the removal of other unwanted proteins. The following protein characterisation methods were used in this study.

2.5.1 Biuret assay

The biuret assay is a colorimetric assay used for protein quantification, based upon the binding of copper ions in the alkaline reagent to the nitrogen atoms of the proteins' peptide bonds (Sapan et *al.* 1999). The copper-protein complex will give rise to a purple colour whose intensity will be proportional to the total protein concentration in the sample, and which can be detected with a spectrophotometer at the peak absorption at 540 nm. The recovery of total protein can then be calculated with the following formula:

$$\text{Total protein recovery (\%)} = \frac{\text{Total units in purified fraction} \times 100}{\text{Total units in previous fraction}} \quad (1),$$

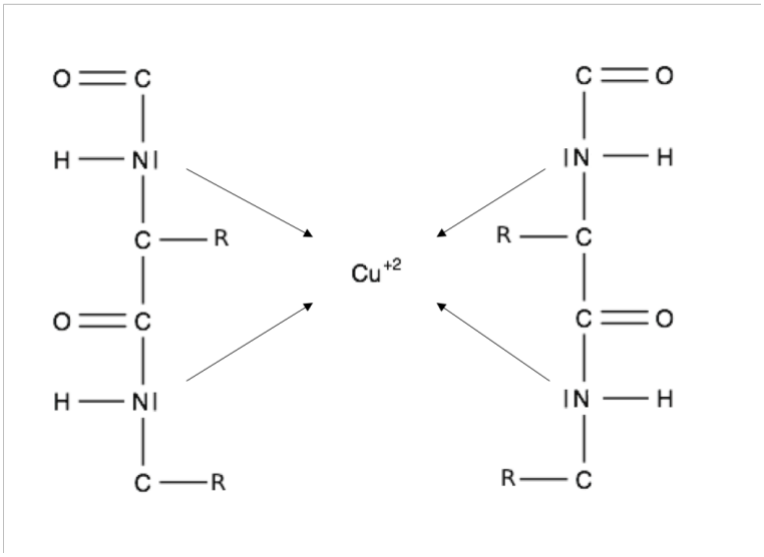

Figure 2. Schematic drawing of the reaction in the biuret assay. Copper ions (Cu^{2+}) in the reagent will react with the nitrogen atoms (N) of a peptide bond. At least two peptide bonds with two nitrogen atoms are required in order for the reaction to take place.

2.5.2 Sodium dodecyl sulphate-polyacrylamide gel electrophoresis (SDS-PAGE)

Sodium dodecyl sulphate-polyacrylamide gel electrophoresis (SDS-PAGE) is a semi-quantitative method for estimating the identity and purity of proteins in a sample by separating them through a gel matrix. Sodium dodecyl sulphate (SDS) breaks non-covalent bindings, unfolding the protein into flexible polypeptide chains. The denaturing agent also generates an equally distributed negative charge to the polypeptides, ensuring a constant mass-to-charge ratio. An electric field forces the polypeptides to migrate towards the anode, and components with shorter peptide length migrate faster through the gel than higher peptide length polypeptides (Shapiro et *al.* 1967). β-mercaptoethanol can be added to the sample to further break the disulphide bonds, thus ensuring complete unfolding.

2.5.3 Size exclusion-high performance liquid chromatography (SE-HPLC)

To identify proteins in a complex sample, size exclusion-high performance liquid chromatography (SE-HPLC) can be used. This technique separates particles in regard to their molecular weight, as the stationary phase beads of the column contain pores of known cut-off size. An aqueous buffer is used as the mobile phase. Small size components can penetrate the pores of the stationary phase beads and will thus be retained, whilst larger size components will elute faster (Lathe & Ruthven 1956). Therefore, the retention time of the different components will be in accordance to their size, and a chromatogram can be obtained by measuring the protein absorbance at 280 nm due to the aromatic rings of tyrosine and tryptophan.

2.5.4 Liquid chromatography tandem mass-spectrometry (LC-MS/MS)

Another orthogonal method of identifying proteins in a complex sample is liquid chromatography-tandem mass spectrometry (LC-MS/MS). In this method, the proteins in the sample are first digested into peptides with a protease such as trypsin or pepsin. The peptides

are separated with liquid chromatography and then ionized to generate charges. The peptides will then migrate through a series of analysers under high vacuum. Mass spectrometry uses the mass-to-charge ratio of ions in gas phase to identify the amount and compounds in the sample, and the analysers sorts the ions according to their mass-to-charge ratio. The result is an experimental mass spectrum, "Fingerprint", of the components in the sample (Pappin et *al.* 1993).

2.5.5 Dynamic light scattering (DLS)

In order to estimate the particle size distribution of proteins in a solution, dynamic light scattering (DLS) can be utilized. DLS uses the Stokes-Einstein equation to evaluate the hydrodynamic diameter of a spherical particle by measuring the translational diffusion coefficient *D* (m^2/s) as the particles fluctuate in the transmitted light (Shiba et *al.* 2010). For non-spherical particles, e.g. Igs, the measurement generates a hydrodynamic diameter equivalent to a sphere with the same translational diffusion coefficient. The measurement may provide particle size distributions based on the intensity of scattered light, particle volume and number.

2.6 Virus-removal nanofiltration

In connection to the virus removal nanofiltration flux determination, cryoporometry by differential scanning calorimetry, nitrogen gas sorption porometry and PFU end-point titration were used. In the characterization of a nanofilter the most critical parameter is the size distribution of pores as it directly relates to the filters' performance to separate particles of a certain size. In this thesis, the pore size distribution was analysed with two different methods, i.e. cryoporometry by differential scanning calorimetry (CP-DSC) (Landry 2005) and with the Barret-Joyner-Halenda (BJH) method derived from nitrogen gas sorption porometry (NGSP) isotherms (Barrett & Joyner 1951).

2.6.1 Cryoporometry by differential scanning calorimetry (CP-DSC)

With CP-DSC it is possible to calculate the pore size of a porous material based on the melting point depression of a liquid inside the pore, as the method utilizes the fact that liquid confined in a pore will freeze and form ice crystals as well as liquid not undergoing phase transition during freezing or melting (Landry 2005). The porous material is soaked in a liquid, frozen and then thawed, and the melting point depression ΔT can then be related to the pore radius r_p with the following equation:

$$\Delta T = \frac{A_m}{r_p - \delta_m} + B_m \qquad (2),$$

where ΔT is the difference between the peak maximum for the melting of water inside the pore and the peak value for melting of the bulk water. A_m, B_m and δ_m are liquid-dependent constants for water, determined as A_m=19.082, B_m=-0.1207 and δ_m=1.12 (Landry 2005).

2.6.2 Nitrogen gas sorption porometry (NGSP)

NGSP is an analysis based on the sorption of nitrogen onto solid surfaces at liquid nitrogen temperature. With this method sorption isotherms, i.e. the amount of gas adsorbed as a function of the relative pressure ($p/p0$), are derived. Prior to the measurement, the sample must be outgassed with vacuum in order to remove any physiosorbed species from the surface that otherwise might interfere with the analysis. The sample is then exposed to a gradually increasing pressure (relative pressure) of nitrogen gas to induce physisorption. As the relative pressure is increased more molecules become adsorbed on the material until eventually nitrogen condenses into a liquid inside the pores, giving a steep rise in the isotherm. When the relative pressure is lowered in the reverse direction during desorption, the pores are emptied from liquid nitrogen in a consecutive order from large pores to small ones. Therefore, the desorption branch of the isotherm can be used to generate a pore size distribution using the BJH method (Barrett & Joyner 1951).

2.6.3 PFU end-point virus titration

There are different methods to validate the performance of the filter using model viruses, including quantitative polymerase chain reaction (qPCR), Tissue cell infectious dose (TCID50) and Plaque forming units (PFU) methods. qPCR method is less commonly used for validations because it cannot distinguish between infective virus particles and nucleic acid fragments. For this reason, TCID50 and PFU methods are preferable. Both methods are based on serial dilutions of a virus sample and the detection of appearing cytopathic effects in a liquid medium or plaque forming units on agar plates cultivated with bacteria. The PFU assay measures the number of virus particles that form plaques (expressed per volume unit) of bacteria cultured on agar plates. In TCID50 assay, each virus dilution is replicated multiple times, and the titer is calculated from the end-point where 50% wells of each replicate are infected (Reed & Muench 1938). The use of TCID50 assay in virus quantification usually require a lab with BSL-2 as it tests mammalian viruses. In this thesis, PFU end-point titration method was used to validate virus clearance, which utilises bacteriophages as model virus and requires only BSL-1 for quantification. The bacteriophage ΦX174 was used as model small-size virus with a size of 28 nm and pI of 6.6, and the host cell was *E. coli*.

Before filtration, PFU end-point titration is done to determine a virus titer for the feed, and after filtration, virus quantification with of the feed and filtrate is done in order to assess an LRV. The number of plaques formed on each agar plate for each dilution is counted and the virus titer (PFU ml^{-1}) is calculated with the following formula:

$$\log_{10}\left(\frac{\text{PFU}}{\text{mL}}\right) = \log_{10}\left(\frac{\text{number of plaques}}{0.1 \times \text{dilution factor}}\right) \qquad (3),$$

where 0.1 is the added volume of virus in ml.

The effectiveness of the clearance method to remove virus is expressed as the $\log_{10}$ virus retention value (LRV) and is estimated with the following formula:

$$\text{LRV} = \log_{10}\frac{\text{PFU (feed)}}{\text{PFU (filtrate)}} \qquad (4),$$

where PFU (feed) and PFU (filtrate) are the calculated virus titers of the feed and filtrate, respectively. If no plaques can be detected in the sample, the theoretical end-point is calculated. The limit of detection in the current experimental set up was ≤ 0.7 PFU ml^{-1}, which corresponds to one detectable plaque in one agar plate for duplicate samples without dilution by assuming that each plaque is produced by one bacteriophage.

2.7 Project aims

In this thesis, the feasibility of virus removal from IgY samples by nanofiltration with millefeuille filter paper is investigated. IgY is isolated from chicken eggs by consecutive crude fractionation and polishing chromatography steps. Following the nanofiltration with millefeuille filter paper, the obtained protein product is then analysed with a range of protein characterisation techniques to assess the purity of the final product and quantify protein yield. To assess the virus clearance properties, the product of IgY isolation and purification is spiked with ΦX174 bacteriophage as model small-size virus and the efficiency of virus removal is expressed as LRV. Figure 3 provides the flow-chart of the project.

2.7.1 Project overview

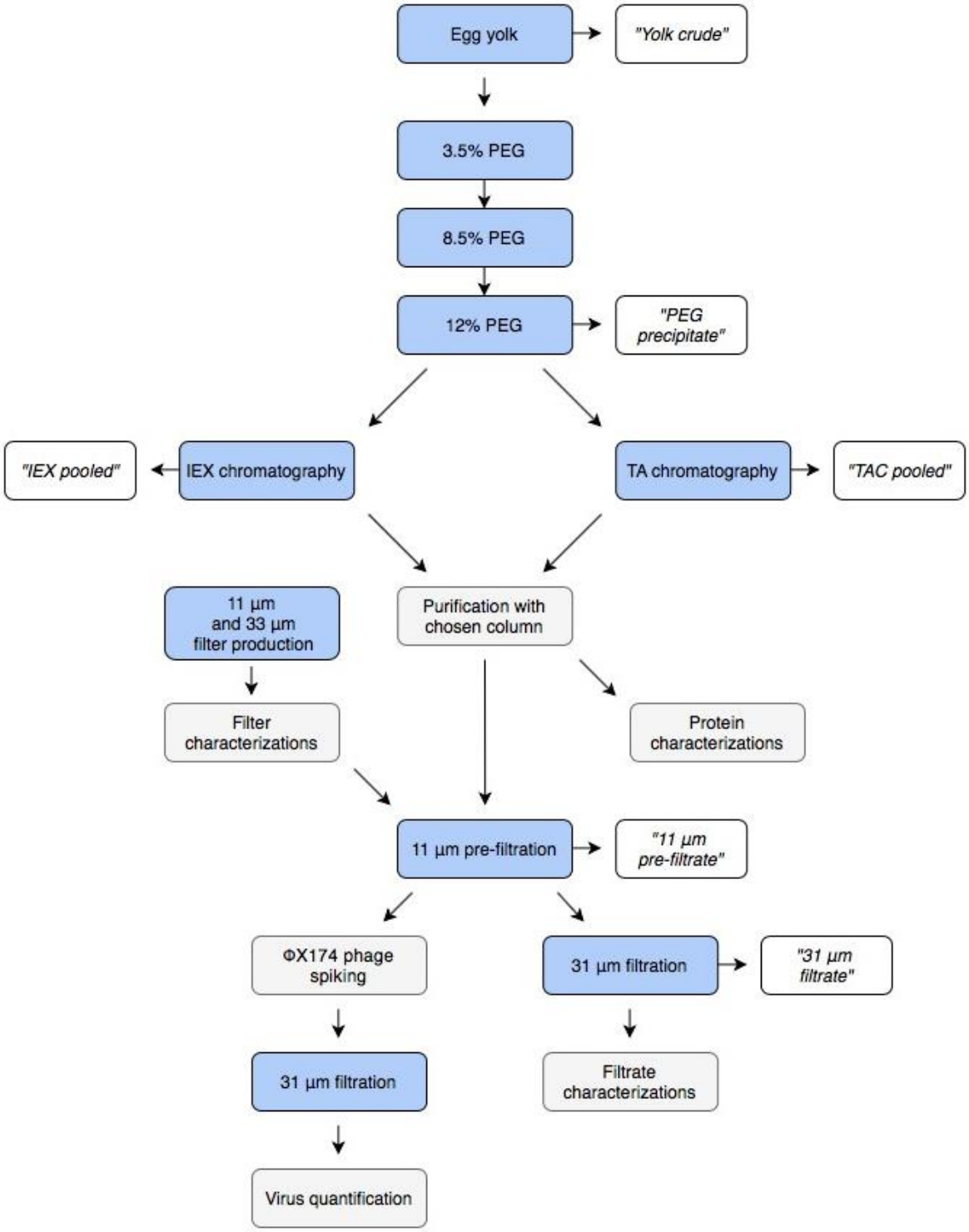

Figure 3. Overview of the project scheme.

3 Materials & Methods

3.1 Materials

Cladophora cellulose was provided from FMC BioPolymer G-3095-10 batch, USA. Support membranes were purchased from Ahlstrom-Munksjö. Eggs from Uggelsta ägg were purchased from Ica Nära Hörnan in Uppsala. Polyethene glycol (PEG-6000), tris-HCl, sodium phosphate dibasic and sodium phosphate monobasic were purchased from Sigma-Aldrich. The columns used in the polishing chromatography were a HiTrap® DEAE 1 ml column and a HiTrap® IgY Purification column purchased from GE Healthcare. Mini-PROTEAN TGX precast protein gels, Precision Plus ProteinTM Dual Colour Standard, 4x Laemmli sample buffer and Tris/Glycine/SDS running buffer for the SDS-PAGE analyses were provided from Bio-Rad. Analytical SE-HPLC was performed with a bioZen 1.8 m SE-3 column from Phenomenex. Bovine serum albumin (BSA), PBS, sodium chloride, 2-propanol, Total Protein Reagent and β-mercaptoethanol were purchased from Sigma-Aldrich. Human intravenous immunoglobulin (hIVIG) is a human-derived liquid preparation of mainly IgG and was a gift from CSL Behring, Australia. Bacteriophage ΦX174 and Escherichia coli (*E. coli*) Castellani and Chalmers strain C were purchased from the American Type Culture Collection (ATCC). Agar was provided from BD. For the Luria-Bertani (LB) broth, sodium chloride was purchased from Sigma-Aldrich, and tryptone and yeast extract were purchased from Thermo Fischer Scientific.

3.2 Methods for isolation & purification of IgY

3.2.1 Crude isolation by PEG precipitation

The egg yolk was separated from the white and transferred to a Munktell filter paper, and then carefully rinsed with deionized water in order to remove any remains of the white. The egg sack was punctured with a pipette tip and the yolk transferred to a 50 ml Falcon tube. PBS (pH 7.4) was added to the tube to a double volume of yolk. Three and a half % (3.5%) PEG of the total volume was added, the tube was vortexed, rolled for 10 min before centrifugation at 5000 rpm for 40 min with a Sorvall ST16 centrifuge. Following the centrifugation, the supernatant was filtered through a Munktell filter paper and transferred to a new 50 ml Falcon tube. Additional 8.5% PEG of the total volume was added, the tube was vortexed and shaken until the polymer was dissolved, then centrifuged at 5000 rpm for 40 min. Following centrifugation, the supernatant was discarded, and the pellet was dissolved in 10 ml PBS buffer with a glass stick and mixed by vortexing. Upon complete dissolution, 12% PEG of the total volume was added, the tube was shaken and vortexed until the polymer was dissolved. The mixture was centrifuged at 5000 rpm for 40 min. The supernatant was discarded, and the pellet was dissolved in 1 ml PBS. Table 2 shows the general protocol for precipitation with PEG per tube and yolk (15 ml).

Table 2. Protocol for the PEG precipitation per tube and egg yolk (15 ml). *"Yolk crude" = Yolk + 2:3 PBS

Yolk [ml]	"Yolk crude"* [ml]	3.5% PEG [g]	Supernatant [ml]	8.5% PEG [g]	Pellet in PBS [ml]	12% PEG [g]	Pellet in PBS [ml]
15	40	1.58	32	2.72	10	1.2	1.2

3.2.2 Polishing chromatography

3.2.2.1 TAC

A HiTrap® IgY Purification (5 ml) column (GE Healthcare) was used on ÄKTA™ Start system with Unicorn software (GE Healthcare) to monitor the absorbance at 280 nm and conductivity of the column effluent. According to the manual of the manufacturer, the column capacity amounted to 100 mg of IgY per column (5 ml). The buffers used in the chromatography were compliant with the recommendation of the manufacturer. The binding buffer was 20 mM sodium phosphate and 0.5 M potassium sulphate (pH 7.4), and the elution buffer consisted of 20 mM sodium phosphate (pH 7.4). For tightly bound proteins that did not elute with the elution buffer, a washing buffer constituting of the elution buffer with 30% 2-propanol was used. The sample load volume was 1 ml. Prior to the injection, the sample was adjusted to 0.5 M of potassium sulphate and then filtered through a 0.45 µm filter. A flowrate of 5 ml min^{-1} was used throughout the entire run. The column was equilibrated with 25 ml of binding buffer, and 1 ml of sample was then passed through the column. Binding buffer at a volume of 25 ml was then applied for the washout of unbound followed by a 25 ml linear gradient from binding to elution buffer. Elution buffer with 30% 2-propanol was applied to the column in order to elute tightly bound proteins from the column until the absorbance returned to baseline. The eluted fractions were collected with the use of an automated fraction collector at a volume of 5 ml each. Prior to pooling of the fractions, the content of the fractions was analysed with SDS-PAGE and the total protein concentration was measured with the biuret assay.

3.2.2.2 IEX

A HiTrap® DEAE 1 ml column (GE Healthcare) was used with ÄKTA™ Start system equipped Unicorn software (GE Healthcare) to monitor the absorbance at 280 nm and conductivity of the column effluent. According to the manufacturer, the column capacity amounted to 100 mg of protein per column. A flowrate of 1 ml min^{-1} was used in accordance to the manufacturer's manual. The binding buffer was 20 mM tris-HCl (pH 8.5), and the elution buffer consisted of the binding buffer and 1 M sodium chloride (pH 8.5). Prior to sample injection, the sample was passed through a 0.45 µm filter. The column was equilibrated with 25 ml of binding buffer, followed by a linear gradient of elution buffer. The eluted fractions were collected with an automated fraction collector at volumes of 1 ml each. Qualitative and quantitative analyses of the protein content were performed with reduced SDS-PAGE and the biuret total protein assay.

3.3 Protein characterizations

3.3.1 Biuret assay

The recovery of total protein after each step in the purification and filtration process was determined with the biuret assay. Total protein reagent was used at a volume ratio of 1:3 and the absorbance of the mixture was detected at 540 nm with the use of a Tecan M200 spectrophotometer. Bovine serum albumin was used in a concentration range of 0.625-4 mg ml^{-1} as a standard curve. All measurements were done in duplicates. The recovery of total protein was calculated with the use of formula (1).

3.3.2 SDS-PAGE

For qualitative analysis of the protein samples, SDS-PAGE was performed on 10% precast stain-free polyacrylamide gels under reduced and non-reduced conditions. The samples were diluted with Laemmli buffer at a volume ratio of 1:4. For reduced conditions, 1 ml of β-mercaptoethanol was added per 100 ml of sample and then heated at 100°C for 10 min to break disulphide bonds. The samples were then separated electrophoretically through the gels at 120 V for 60 min. The detection was performed with a ChemiDoc XRS+ system equipped with ImageLab analysis software. Precision Plus ProteinTM Dual Colour Standard was used as standard marker.

3.3.3 DLS

Dynamic light scattering (DLS) was performed in order to estimate the particle size distribution of the samples before and after the purification and filtrations steps. The measurements were done in 1 ml standard cuvettes with the use of a Malvern Mastersizer 3000. All measurements were done in triplicate.

3.3.4 SE-HPLC

SE-HPLC analysis was performed with a Hitachi Chromaster HPLC-UV and a BioZen 1.8 µm SEC-3 column. The mobile phase consisted of 10 mM sodium phosphate (pH 6.8) and the flow rate was 0.3 ml/min. The absorbance intensity was monitored at 280 nm. Prior to the analysis, the samples were centrifuged at 10 000 rpm for 5 min and then filtrated through a 0.2 µm filter.

3.3.5 LC-MS/MS

For mass spectrometry, the 31 µm filtrates were analysed by in-solution digestion with trypsin according to standard operation procedure and then analysed by LC-Orbitrap Tandem mass spectrometry (MS/MS) at the MS Facility at Uppsala University.

3.4 Filter preparation and characterizations

3.4.1 Filter preparation

The *Cladophora* cellulose dispersion was produced in a LM20 microfluidizer, by passing the material through hole-sized chambers at a pressure of 1800 bar. The filters were then prepared by draining dispersion in Buchner funnels on top of support membranes soaked in deionized water with the use of vacuum. The filters were dried in a hot-press (Rheinstern) at 105°C for 3 h and then cut to a diameter of 47 mm with a cutting press (Mäder pressen).

3.4.2 Thickness & basis weight

The thicknesses of the produced filters were measured with a digital calliper (Mitutoyo Absolute). Each filter was measured at ten different spots to calculate the mean thickness. To derive the basis weights (g m^{-2}), the filters were weighed on an analytical balance (Mettler Toledo).

3.4.3 Hydraulic flux

Flux measurements were performed with filter holders (KST-47) from Advantec and a balance (Mettler Toledo MS1602TS/00 Precision Balance) supplied with the LabX software (Mettler Toledo) to monitor the weight change of the filtrate over filtration time. For the measurement's hydraulic permeability, deionised water was filtered at a load volume of 57.47 L m^{-2} (100 ml) at 1 bar.

3.4.4 CP-DSC

In order to estimate the pore size distribution of the produced filters, cryoporometry by differential scanning calorimetry (CP-DSC) was performed with the use of a Mettler DSC3 instrument equipped with STRARe software. The filters were cut into strips, weighed and then soaked in deionized water overnight. The day before the measurement each strip was folded and then placed in an aluminium pan with a lid. The pan was then placed in the auto-sampler of the instrument for measurement. The sample was frozen from -30℃ at a rate of -10 K min^{-1} and then subsequently heated to 15℃ at a rate of 0.7 K min^{-1}. The measurement generated two endothermal peaks, representing the melting points of the water confined inside the pores (2-50 nm range) and bulk water (outside pores). The difference in melting point was used to calculate the pore size with formula (2).

3.4.5 NGSP

From nitrogen gas sorption isotherms, the pore size distributions of the filters could be determined from the Barret-Joyner-Halenda (BJH) method and the use of ASAP2020 (Micromeretics) instrument. One day before the measurement, the filters were cut in strips and then folded to fit in a sample tube. Prior to analysis, the samples were outgassed in vacuum at 95℃ for 6 h. The pore size distribution could then be calculated using the BJH method, from the desorption branch of the isotherm.

3.5 Nanofiltration

In the pre-filtration, the feed was "TAC pooled" fraction adjusted to a concentration of 1 mg ml^{-1}. The feed was filtered at a load volume of 14.41 L m^{-2} (25 ml) at a transmembrane pressure (TMP) of 1 bar. The product of feed filtration will be referred to as "11 µm pre-filtrate". In the 31 µm filtration, the pre-filtrate was filtered at a TMP of 3 bar, and the resultant product will be referred to as "31 µm filtrate". All filtrations were done in triplicate, and control samples were held before each filtration in order to calculate the recovery of proteins. Prior to the filtrations, deionized water was first filtered at a TMP of 1 bar in order to wet the filter and flatten out eventual wrinkles on the filter that could arise. V_{max} was calculated in order to get the maximum load volume of the feed solutions before fouling of each filter. V_{max} was obtained

through linear regression, as the inverse of the slope from plotting time over the filtrate load volume (t/V).

3.6 Virus titration

ΦX174 (28 nm; pI 6.6) phages were used as model small-size virus for the virus removal filtration. The virus was propagated in *E. coli* Castellani and Chalmers strain C. To determine the bacteriophage titer, *E. coli* was cultured in Luria-Bertani (LB) broth in a shaking incubator (INCU-LINE ILS4) at 37℃ at 220 rpm for 2 h.

The feed solution ("11 μm pre-filtrate") was spiked with the ΦX174 phage at a concentration of 6.0 ±0.6 PFU ml^{-1}, and the filtration was performed at a TMP of 3 bar at a load volume of 14.41 L m^{-2} (25 ml). A 500 μl fraction of the feed solution was held as control sample to check the difference in phage titer of the feed and filtrate. The filtrations were done in triplicate and the virus quantification of each filtrate was done in duplicate.

After the virus removal filtration, the phage titers of the feed and filtrate solutions were evaluated using PFU end-point titration. The feed solution was serially diluted up to 10^{-6} with LB broth using a liquid handling robot (Tecan Freedom EVO 75, Austria). The feed and filtrate solutions were mixed with *E. coli* and soft agar, then poured onto the surface of petri dishes prepared with hard agar. The agar plates were incubated at 37℃ for 5 h. The bacteriophage titers were calculated with formula (3), and the retention of the virus removal filtration could then be estimated using formula (4).

4 Results & discussion

4.1 Crude isolation by PEG precipitation

Table 3 shows the mean and standard deviation of the total protein concentration measured with the biuret assay of all three batches (B1, B2 and B3) of the PEG precipitation method for crude fractionation of IgY. The result shows that the total protein concentration differs between the batches, with 56.0±0.02 mg ml^{-1} as the highest concentration (B1) and 40.9±0.06 mg ml^{-1} as the lowest (B3). Figure 2 shows the result of the non-reduced and reduced SDS-PAGE analysis of B1, B2 and B3. The lanes representing B1, B2 and B3 under non-reduced conditions contain one intense band between 150 and 250 kDa, which could be due to monomeric IgY. The lanes representing B1, B2 and B3 under reduced conditions all contain one intense band around 65 kDa and two bands between 25 and 30 kDa, which could be due to IgY heavy chain (IgY-HC) as well as kappa and lambda IgY light chains (IgY-LC), respectively. Additional bands in the lanes of reduced samples can be seen at approximately 75, 40, 35 and 10 kDa, which resemble results of other studies after PEG precipitation which could also report IgY purities around 80% (Al-Razem et *al.* 2018; Pauly et *al.* 2011).

Table 3. The mean and standard deviation of the total protein concentrations of the final PEG precipitates (n=3) measured with the biuret assay. IgY purity** was estimated semi-quantitatively by measuring the band intensities of IgY in the reduced SDS-PAGE analysis gel. IgY recovery** was calculated based on the purity estimations.

Batch	Total protein concentration [mg ml^{-1}]	IgY purity* [%]	IgY recovery** per 15 ml egg yolk [mg]
B1	56.0±0.02	94	63
B2	53.8±0.01	96	62
B3	40.9±0.06	93	52

Other studies have reported highly varying IgY recoveries after PEG precipitation, e.g. 130-132 mg (Deignan et *al.* 2000), 40-80 mg (Pauly et *al.* 2011) and 74 mg (Akita & Nakai 1993) per egg yolk (15 ml) with corresponding purities of 89% (Deignan et *al.* 2000) and 80% (Pauly et *al.* 2011; Akita & Nakai 1993).

Semi-quantitative analysis of the protein bands in the gel obtained by SDS-PAGE (Fig. 4), suggest that the purity of IgY amounted to 93-96% which generates corresponding recoveries of 52-63 mg of IgY per egg yolk (15 ml), and are within the range of the recoveries reported after PEG precipitation by other sources. The purity estimation is likely overrated, as the band intensity of IgY-HC especially is oversaturated.

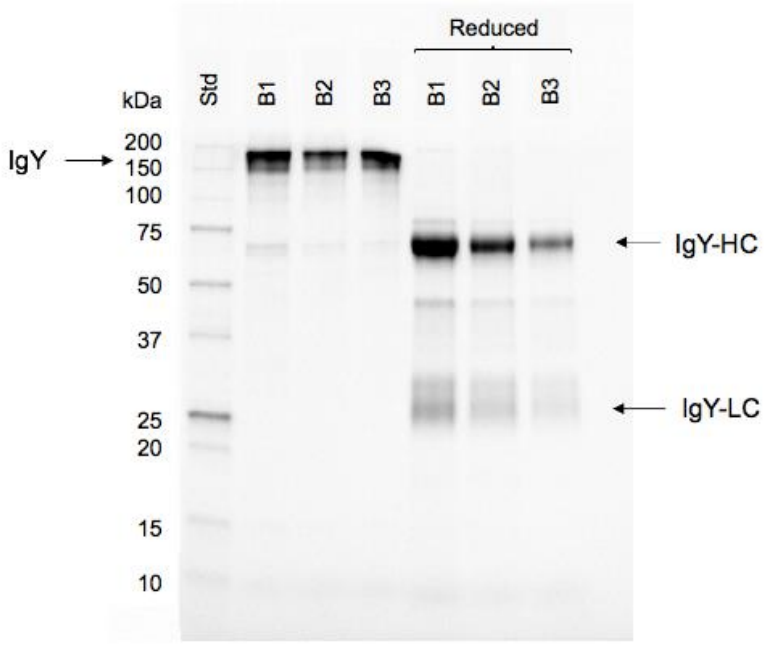

Figure 4. Gel obtained from non-reduced and reduced SDS-PAGE analysis of PEG precipitation batches B1, B2 and B3 with 200-fold dilutions.

4.2 Polishing chromatography

4.2.1 TAC

Figure 5 represents the combined chromatograms of three runs with 1 ml of the protein sample ("PEG precipitate") applied to the HiTrap® IgY Purification column. The figure shows three different groups of peaks. The first peak (1) represents the washout of proteins that have not bound to the column with binding buffer. The second peak (2) represents the elution of column-bound proteins with elution buffer, and the third peak (3) shows the proteins that are tightly bound to the column and elute after the addition of elution buffer with 30% 2-propanol. The figure also shows the fractions in tubes T4-T15 collected during the runs. Since 2-propanol was used for the elution of column-bound proteins that were tightly bound to the column also after elution with elution buffer, the corresponding collected fractions were not pooled since the organic solvent is likely to have a denaturing effect on the proteins.

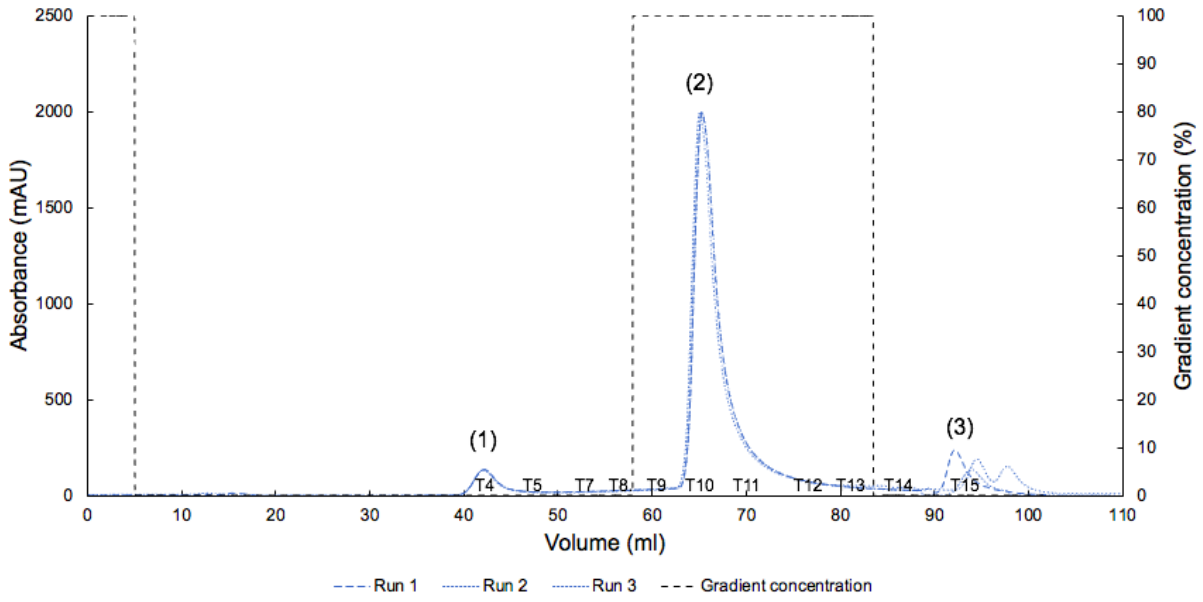

Figure 5. Chromatogram from three runs with the HiTrap® IgY Purification column. The peaks represent the washout of unbound (1), elution of column- bound (2), and elution of column-bound with 30% 2-propanol.

Table 4 shows the mean amount of proteins found in the collected fractions from the runs (n=3). The total amount of protein that was collected after the chromatography amounted to approximately 75% of the initial total protein amount in the 1 ml sample. In total, 68% of the total amount of injected protein was column-bound, eluted and found in the collected fractions under peak (2) in Figure 5. Approximately 2.7 % of the total amount of protein did not bind to the column, represented by peak (1) in Fig. 5, and 4.1% were too tightly bound to the column and required 2-propanol in order to elute.

Table 4. Mean and standard deviation of total protein quantity (mg) and percentage in the initial sample and collected peak fractions from the runs (n=3). (1): Washout of unbound; (2): Column-bound; (3): Washout of column-bound with 30% 2-propanol.

	Quantity [mg]	Quantity [%]
Initial protein	53.8	100
(1) Washout of unbound fraction	1.4±0.7	2.7±0.01
(2) Column-bound fraction	36.9±2.8	68.6±0.03
(3) Washout of column-bound fraction	2.2±2.7	4.1±0.03
Total protein in collected fractions	40.5±3.1	75.4±0.03

Figure 6 shows the gel obtained from the reduced SDS-PAGE analysis of the collected T4-T15 fractions with the HiTrap® IgY Purification column. The lanes, representing T5-T15 pooled fractions, show one band at approximately 65 kDa, which most likely is IgY heavy chain (IgY-

HC), and two bands between approximately 25 and 30 kDa, which could be of two types of IgY light chain (IgY-LC), i.e. kappa and lambda. Additionally, three bands can be seen between 35 and 40 kDa. All lanes have also one band around 10 kDa. T10 had the highest amount of protein among pooled samples (Table 3), which is clearly seen from the high intensity of the lanes in the SDS-PAGE analysis. A band at approximately 200 kDa can be seen in lane T10, which could also be present in the other lanes but fails to show because of the low concentration protein at specified dilution. It should be noted that the lane representing T4 (from washout pool) differs from the other lanes, featuring a band at 75 kDa that cannot be seen in the other lanes. The latter suggests that the protein representing the band at 75 kDa was successfully separated from the other proteins. As this protein was most probably not IgY; the fraction containing this protein was not included in the pooling of the fractions.

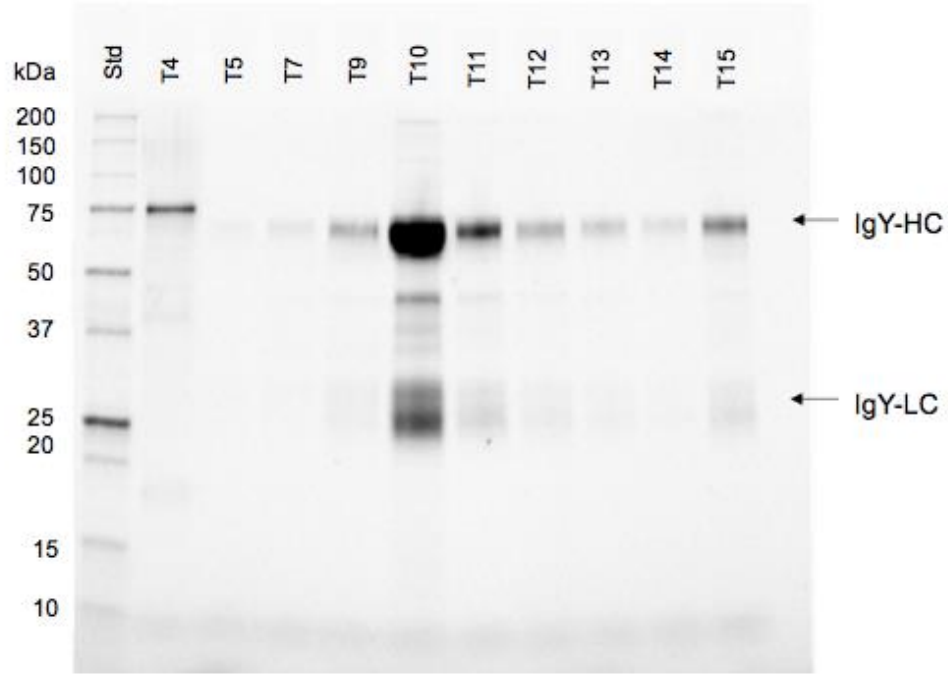

Figure 6. Gel obtained from reduced SDS-PAGE analysis of fractions obtained from one run with 5-fold dilutions.

4.2.2 IEX

Figure 7 shows the combined chromatograms obtained from three runs with the HiTrap® DEAE column as well as the fractions collected in one run. The first absorbance peak in the chromatogram (1) represents proteins that did not bind to the column. The elution buffer was applied to the column at approximately 27 ml and the second peak (2) represents column-bound proteins that were subsequently eluted.

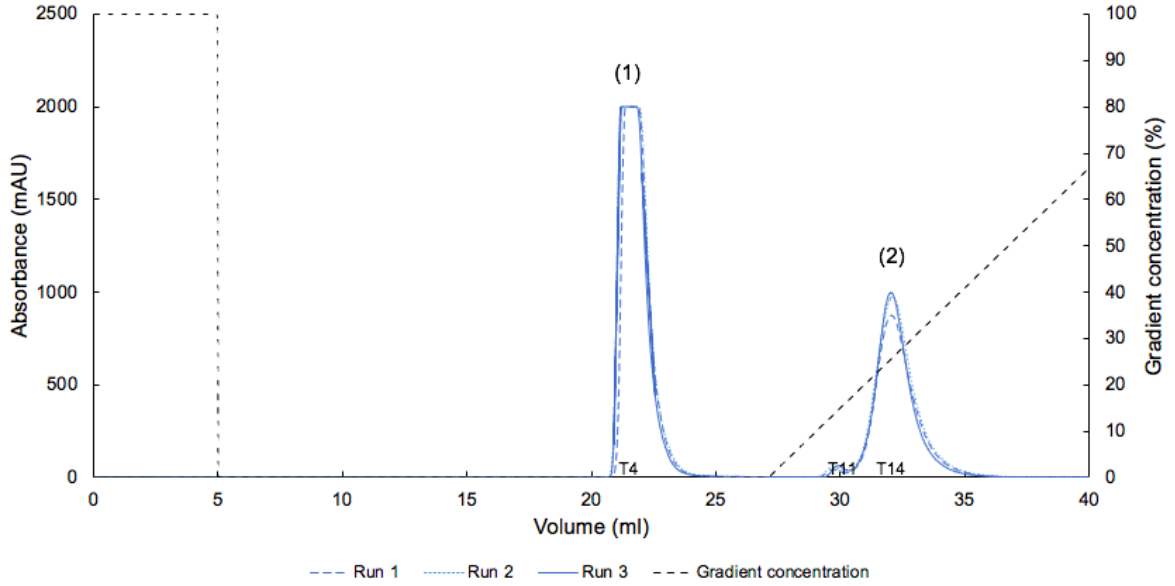

Figure 7. Combined chromatograms from the runs (n=3) with the HiTrap® DEAE Fast Flow column. The peaks represent the washout of unbound with binding buffer (1) and elution of column-bound with elution buffer (2).

Table 5 shows the quantity of protein obtained after chromatography in the pooled fraction of washout of unbound proteins with binding buffer (1) and elution of column-bound proteins with elution buffer (2). In total, 93% of the initial amount of proteins could be found in the collected fractions. Of these, 78% were found in the fractions collected under the first absorbance peak representing the proteins that had not bound to the column, and only 15% of the total amount of proteins were bound to and eluted from the column.

Table 5. Mean and standard deviation of total protein quantity (mg) and percentage in the initial sample and collected peak fractions from the runs (n=3). (1): Washout of unbound with binding buffer; (2): Elution of column-bound with elution buffer.

	Quantity [mg]	Quantity [%]
Initial protein	40.9	100
(1) Washout of unbound fraction	32±1.4	78±0.03
(2) Column-bound fraction	6.1±0.1	15±0.02
Total protein in collected fractions	38.1±1.3	93±0.03

Figure 8 shows the gel image obtained after reduced SDS-PAGE analysis of the peak representing collected fractions. The lanes T4 and T14 represent fractions collected during the washout of unbound (1) and elution of column-bound proteins (2). The results suggest that most proteins did not bind to the column (lane T4), including IgY, which most likely is represented as the intense band around 60 kDa (IgY-HC) and bands between 25 and 30 kDa, i.e. kappa and lambda IgY-LC, respectively. Both lanes show multiple bands between 30 and 40 kDa, as well as around 10, 75, 130 and 200 kDa. Overall, the result from the SDS-PAGE analysis in Fig. 8 resembles that of the result of TA chromatography (Fig. 6), except from the band at 75 kDa which was successfully separated by TA chromatography as seen in Fig. 6.

The separation was acceptable, but the capacity of the column was probably overestimated due to optimistic data from the provider. Thiophilic chromatography was thus the primary choice, but this may still serve as an additional separation step, if required.

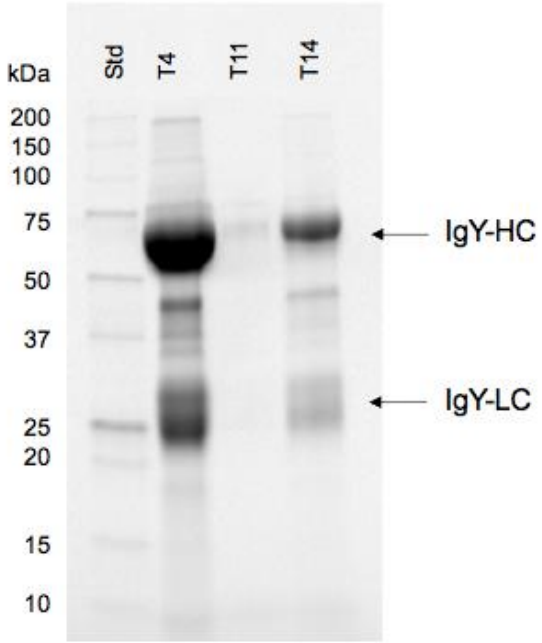

Figure 8. Gel obtained from SDS-PAGE analysis of peak fractions collected from one run with the HiTrap® DEAE column. The fractions were diluted 5-fold.

4.3 Purification of IgY for virus removal filtration

In the previous section, the isolation and purification of IgY was performed in a small scale for analytical purposes. For the virus removal filtration, larger quantity of IgY would need to be isolated and purified using crude isolation by PEG precipitation and polishing TAC.

Table 6 shows the protein recovery following PEG precipitation and chromatography for up-scaled experiment. A final protein recovery of 65% after the chromatography step was observed, which is lower than that observed in the scale-down model, i.e. 69%. The latter is likely to occur due to the microfiltration in the sample preparation since the loss of proteins due to high viscosity increases with an increased number of runs.

Table 6. Total protein concentrations of the samples after each purification step measured with the biuret assay and the recovery of total proteins determined with formula (1).

Sample	Volume [ml]	Total protein concentration [mg ml^{-1}]	Total protein amount [mg]	Recovery [%]
PEG precipitate	8	57.9±0.04	463	100
TAC pooled	120	2.49±0.07	299	65

Figure 9 shows the result of the SDS-PAGE analysis of the fractions from crude yolk (Yolk crude), "PEG precipitate" and the pooled fractions after TA chromatography (TAC pooled) for the purification of IgY for the virus removal filtration. Standard marker (Std) 10-250 kDa and human IVIG (IgG) were included as references. The results show that the band at 75 kDa in "Yolk crude" and "PEG precipitate" is completely removed after chromatography (TAC pooled). The bands in "PEG precipitate" and "TAC pooled" fractions at approximately 65 kDa and 25-30 kDa are assumed to be the heavy chain and lambda and kappa light chains of IgY, respectively (Al-Razem et *al.* 2018; Pauly et *al.* 2011). In addition, several bands in both "PEG precipitate" and "TAC pooled" can be seen between 35-40 kDa as well as bands at approximately 250 and 10 kDa, which have not been removed after chromatography. Because of the different dilutions of "PEG precipitate" and "TAC pooled" due to the high intensity of the band at 65 kDa, it is not possible to establish whether any band has been reduced after chromatography.

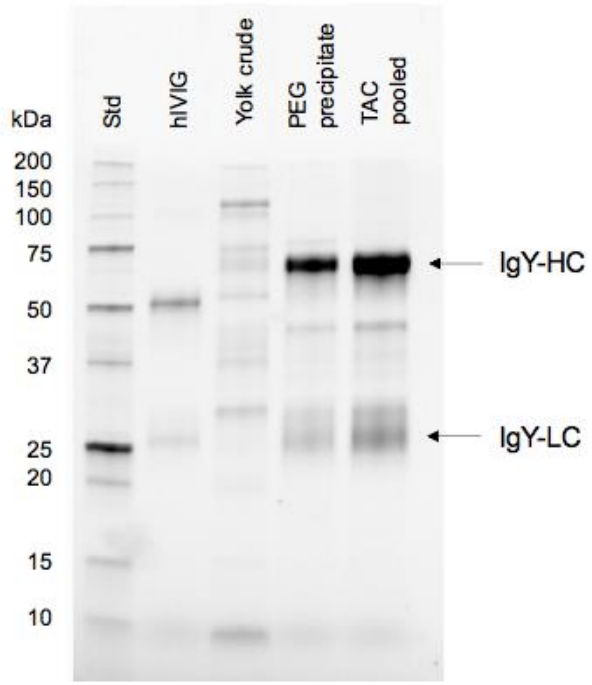

Figure 9. Gel obtained from reduced SDS-PAGE analysis of each step in the purification process, including hIVIG (IgG) and standard marker (Std) as references. Dilutions: "hIVIG" 1:100, "Yolk crude" 1:200, "PEG precipitate" 1:200, "TAC pooled" 1:5.

Figure 10 shows the particle size distribution by intensity measured with DLS of "PEG precipitate" and "TAC pooled" fractions together with a highly purified human IVIG industrial sample containing mainly IgG. The measurement of "hIVIG" gave a distribution peak between approximately 3 and 20 nm, and it is expected that an equally pure sample of IgY would give a similar size distribution. Measurements of both "PEG precipitate" and "TAC pooled" gave a broad distribution peak between approximately 7 and 100 nm (PEG precipitate) and between 7 and 70 nm (TAC pooled). The maximum peak of "PEG precipitate" between 20 and 30 nm has shifted to lower distributions for "TAC pooled". The narrowing of the main peak suggests that some larger species present in the fractions PEG precipitate fraction were removed after TAC. The DLS analysis of the "TAC pooled" fraction further suggests that this fraction is polydisperse as it also generated a second distribution peak between approximately 105-900 nm, which could indicate formation of protein aggregates.

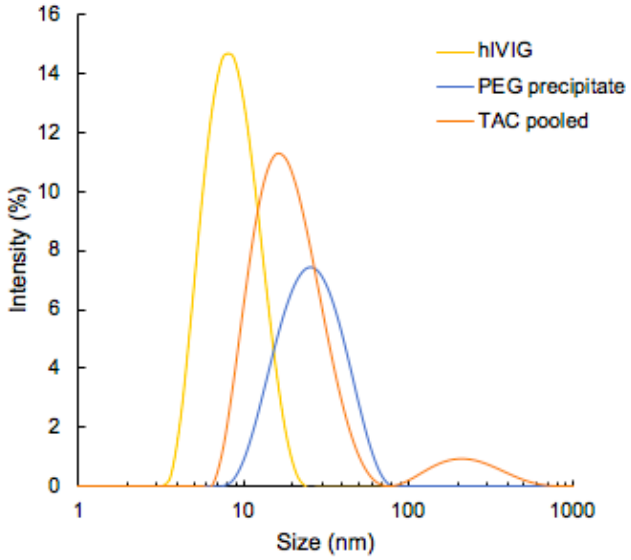

Figure 10. Particle size distributions by intensity of “hIVIG” (IgG), "PEG precipitate" and "TAC pooled" measured with DLS.

4.4 Filter characterizations

In order to characterize the produced filters, the thickness, basis weight, hydraulic flux, and the pore size distribution were analysed. Two variants of the mille-feuille filter were produced, i.e. pre-filters for removing high molecular weight proteins and protein aggregates and dedicated virus removal filters. The pre-filtration was intended to minimize blocking of the pores in the dedicated virus removal filters as it will be discussed below. The pre-filters had a filter thickness of 11 µm, and the dedicated virus removal filters had thicknesses of 31 µm. For detailed discussion on the effect of mille-feuille filter thickness on aggregate removal see (Manukyan et *al*. 2020).

Table 7 shows the mean thickness, basis weight and flux value measured of the filters produced for the pre-filtration and following virus removal filtration. The local variations of thickness were insignificant, and the measured thickness of the filters was within specified range, i.e. 11.1±0.3 µm and 31.1±2.5 µm). The basis weight (g m^{-2}) of the samples reflected the differences in the thickness of the produced samples. The hydraulic flux values amounted to 146±12.5 and 47±4.7 L m^{-2} h^{-1} for the 11 and 31 µm, respectively, and mirror the thickness of each filter type, as a shorter diffusion length will lead to a higher throughput of feed volume per surface area and time.

Table 7. The thicknesses, basis weights and hydraulic flux values of the produced filters (n=3).

	Thickness [µm]	Basis weight [g m^{-2}]	Flux H_2O [L m^{-2} h^{-1}]
Pre-filters	11.1±0.3	12.9±0.7	146±12.5
Virus removal filters	31.1±2.5	29.0±1.6	47±4.2

Figure 11 shows the heat flow curves from the CP-DSC measurements of the produced filters, where the endothermal peaks represent the melting point of the water confined in the pores and the water in the bulk, respectively. It can be seen that there is a shift in the melting point for the pore-constricted water for the 31 µm filters to lower heating rates than that of the 11 µm filters, whereas the melting point for the bulk water is positioned at the same values around 0.7 °C. The difference in melting point temperature between the bulk water and pore-constricted water for the 31 µm filters thus results in a smaller pore size than that of 11 µm with a lower corresponding difference in melting point temperature, as calculated from formula (2) and shown in Table 7.

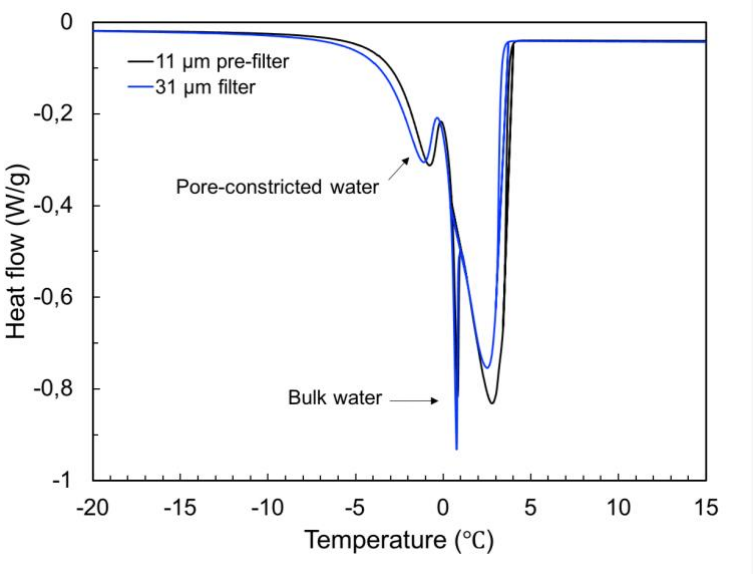

Figure 11. Heat flow curves of the 11 and 31 µm filters from CP-DSC and is typical for all measurements (n=3). The arrows point at the endothermal peaks representing the melting point of the bulk water and the water constricted in the pores, respectively.

Figure 12 shows (a) the cumulative pore size distribution and (b) BJH pore size distribution of the 11 and 31 µm filters. According to the results, the 31 µm filters have a narrower pore size distribution than the 11 µm pre-filters, as expected, with pore size mode at approximately 21 and 24 nm, respectively. The result from the cumulative pore size distribution (a) and BJH method (b) suggests that the 31 µm filters have a lower total pore volume and a larger fraction of smaller pores than the 11 µm pre-filters. For larger pores above 30 nm, the distributions are relatively similar between the 11 and 31 µm filters.

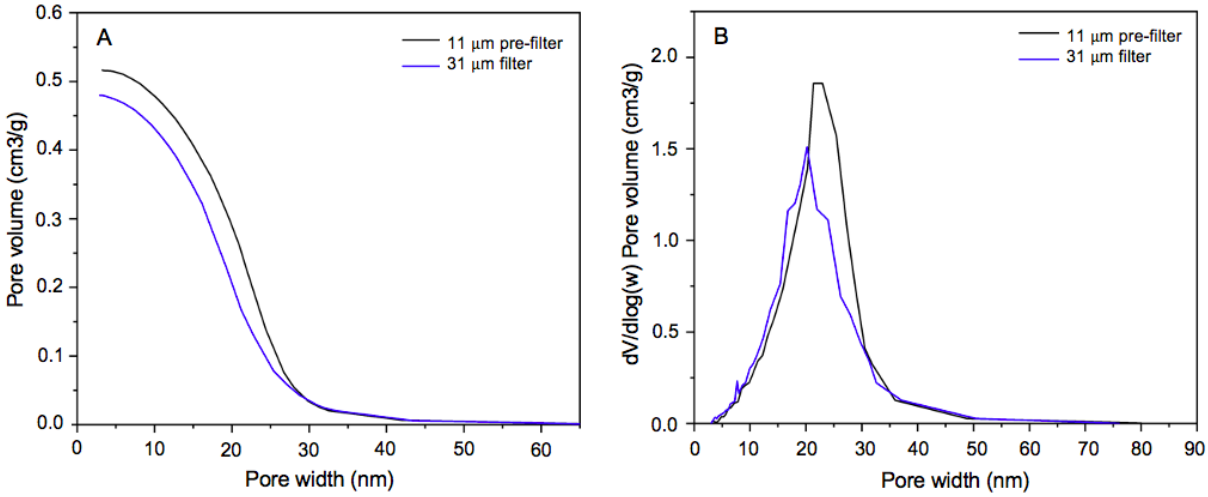

Figure 12. The a) cumulative pore size distribution and b) pore size distribution with the BJH desorption method, of the 11 and 31 µm filters measured from nitrogen gas sorption isotherms.

Table 8 shows the mean pore size mode of the produced filters measured with CP-DSC and BJH method from NGSP isotherms where the pore size mode refers to the position of the highest peak in Figure 10b. The thinner layer of nanofibers of the pre-filters were expected to generate larger pores than that of the filters used for the virus removal with intended thicknesses of 33 µm, which is here confirmed as the pre-filters exhibit pore size mode of 24 and 33.6±2.1, and dedicated virus removal filters 21 and 26.2±2.1 derived from BJH-NGSP and CP-DSC methods, respectively. An important remark on the results of the two methods used to estimate the pore size distribution is that CP-DSC measures the pore mode in wet conditions, whereas the method of NGSP generates a pore size distribution measured when the filters are in a dry state.

Table 8. The pore size distributions of the filters measured with CP-DSC (n=3) and the BJH method from NGSP (n=1).

	Pore size mode [nm]	
	CP-DSC	BJH method-NGSP
11 µm pre-filters	33.6±2.1	24
31 µm filters	26.2±2.1	21

4.5 Filtration of TAC pooled feed solution

To assess the recovery of protein and to monitor the compositional changes before and after the virus removal filtration, two-step filtration was conducted with TAC-pooled feed solution.

Figure 13 shows the mean flux plotted against the load volume (L m^{-2}) from the pre-filtrations with the 11 µm filters (n=3) at 1 bar with "TAC pooled" (1 mg ml^{-1}) as feed solution, and the following filtration with the 31 µm filters (n=3) at 3 bar with "11 µm pre-filtrate" as feed. The rate of fouling in the pre-filtrations is significant as the flux starts with approximately 130 L m^{-2} h^{-1} and ends with 50 L m^{-2} h^{-1}, resulting in an average flux decay of approximately 54% for a load volume of 14.41 L m^{-2}. In the following filtration with the 31 µm filter, some fouling still take place as the flux starts at around 100 L m^{-2} h^{-1} and ends with approximately 85 L m^{-2} h^{-1}. The maximum load volume before fouling takes place (V_{max}) was calculated to 27 L m^{-2} for the 11 µm pre-filters and 90 L m^{-2} for the 31 µm filters. From these results it is clear that the implemented pre-filtration heavily contributed to an enhanced throughput in the following 31 µm filtration.

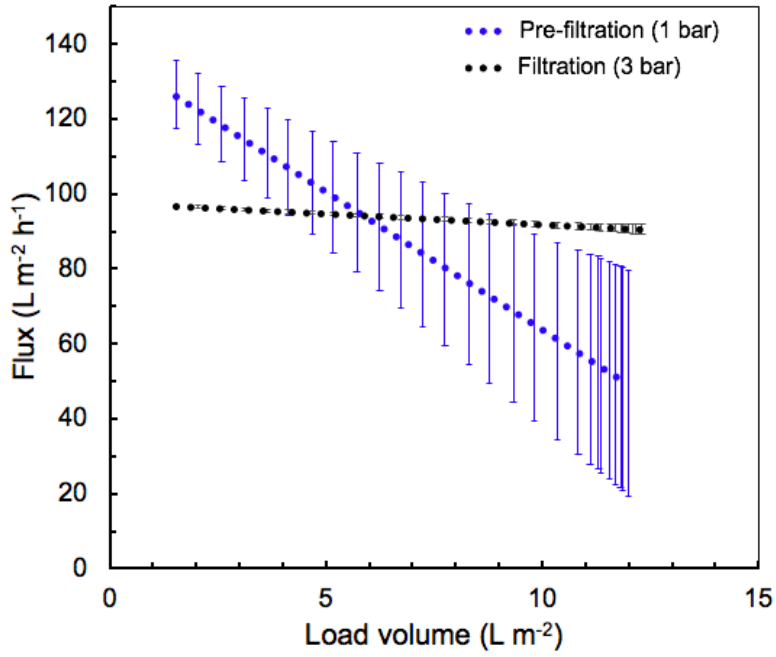

Figure 13. Plot of the mean of flux with standard deviation against the load volume of pre-filtrations (n=3) with "TAC pooled" as feed solution at a total protein concentration of 1 mg ml^{-1}, and filtrations (n=3) with "11 µm pre-filtrate" as feed solution.

4.6 Pre-filtrate and filtrate characterizations

Table 9 shows the total protein concentrations of the fractions from the filtrations measured with the biuret total protein assay. It is seen from the table that the recovery of total protein progressively decreases with each step. The decrease in protein concentration is relatively larger for the pre-filtrate fraction compared to filtrate. The results correlate well with the fouling behaviour observed in Fig. 13 above for pre-filtrate and filtrate samples. In a real downstream process, a range of different pre-filtrations and filtrations are typically implemented to remove various contaminants from the feed. In particular adsorptive depth filtration is used to clear the feed from cell harvest and aggregates which ultimately enhances the throughput of the final virus removal filtration.

Table 9. Total protein concentrations of feed ("TAC pooled") and filtrates measured with the biuret assay.

	Total protein concentration [mg ml^{-1}]	Recovery [%]
Feed (TAC pooled)	0.99±0.01	100
11 µm pre-filtrate	0.83±0.03	83
31 µm filtrate	0.68±0.04	68

Figure 15 shows the result from reduced SDS-PAGE analysis of the feed (TAC pooled), “11 µm pre-filtrate”, and “31 µm filtrate”. Lane “Std” contains the standards marker with proteins ranging from 10-250 kDa. All lanes contain one intense band at approximately 70 kDa, two bands between approximately 25 and 30 kDa, and one band around 10 kDa. Three bands between 35 and 40 kDa can also be seen in all lanes. As the total protein concentration measurements showed (Table 7), there is substantial loss of protein after each filtration step, which is not detectable in the SDS-PAGE result.

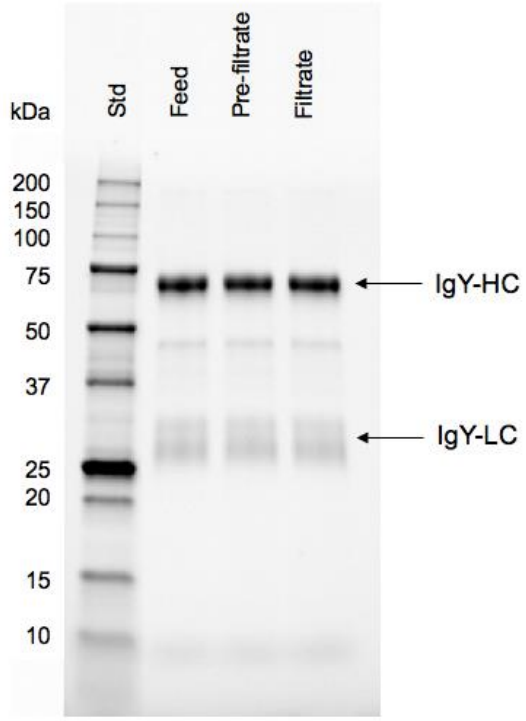

Figure 15. Gel image obtained after reduced SDS-PAGE analysis of the feed (TAC pooled), pre-filtrate and filtrate (n=3) with 5-fold dilutions.

Figure 16 shows the DLS particle size distributions by (a) intensity and (b) volume of the feed solution (TAC pooled), "11 µm pre-filtrate" and "31 µm filtrate" with DLS. In the graph showing the intensity distribution it can be seen that the second peak in the TAC-pooled feed solution disappears after pre-filtration. Furthermore, the particle size distribution narrows for each step, especially clearly seen in the intensity distribution profile. The feed sample features the broadest pore size distribution, whereas 31 µm filtrate shows the narrowest distribution, characterised by a shift of the modal size from 20 nm to 10 nm, respectively. No particles above 30 nm could be detected in the 31 µm filtrate. The latter result is expected as the 31 µm filter according to the filter characterization has a modal pore size around 21-26 nm as determined with both CP-DSC and NGSP (Table 8), thereby generating a molecular cut-off threshold. The results are also compliant with the flux curves as discussed above, where filtrations of "TAC pooled" feed solution through 11 µm pre-filter resulted in rapid flux decay due to protein aggregates (Fig. 13).

It should be noted that no second peak due to protein aggregates was seen in the volume distribution curves of "TAC-pooled" feed sample in Fig. 16b. This suggests that the concentration of aggregates in "TAC pooled" feed solution is very small and thus the majority of the particles have size distribution peaks ranging from 6 to 50 nm, with a maximum peak around 10 nm. The size distribution by volume becomes progressively narrower and the peak position shifts to smaller sizes.

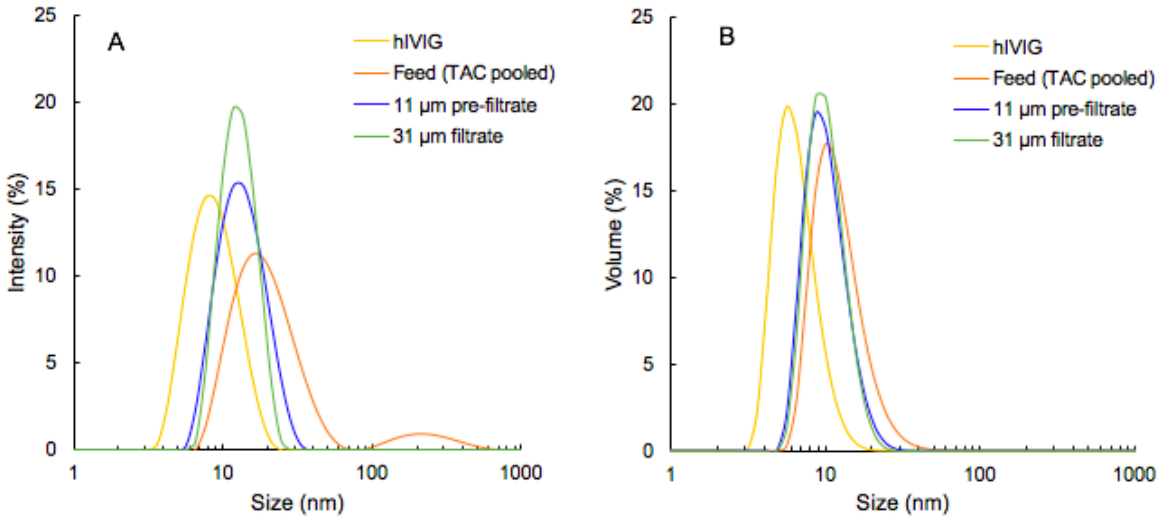

Figure 16. The size distributions of hIVIG (IgG), feed (TAC pooled), pre-filtrate and filtrate by a) intensity and b) volume, measured with DLS (n=3).

Analytical SE-HPLC was performed to further analyse the differences between the samples as shown in Fig. 16. Figure 17 shows the combined SE-HPLC profiles of the feed solution (TAC pooled), "11 µm pre-filtrate" and "31 µm filtrate". The arrow marks the retention time for "hIVIG" (t_R=9.7 min). The profile is characterised by multiple overlaying peaks, which suggest a complex mixture of proteins in the sample. Similar to SDS-PAGE analysis no loss of any specific molecular weight fraction of protein has occurred. In general, the overall absorbance intensity decreased for each filtration step. According to previously published literature, the small peak at a retention time of around 6 min likely represents IgY dimer, and the main peak at around 9 min monomeric IgY (Sahlin et al. 2016; Kim & Patterson 2003). Based on the profile it is clear that other impurities are present in the sample, represented by intensity peaks for retention times between 10 and 20 min.

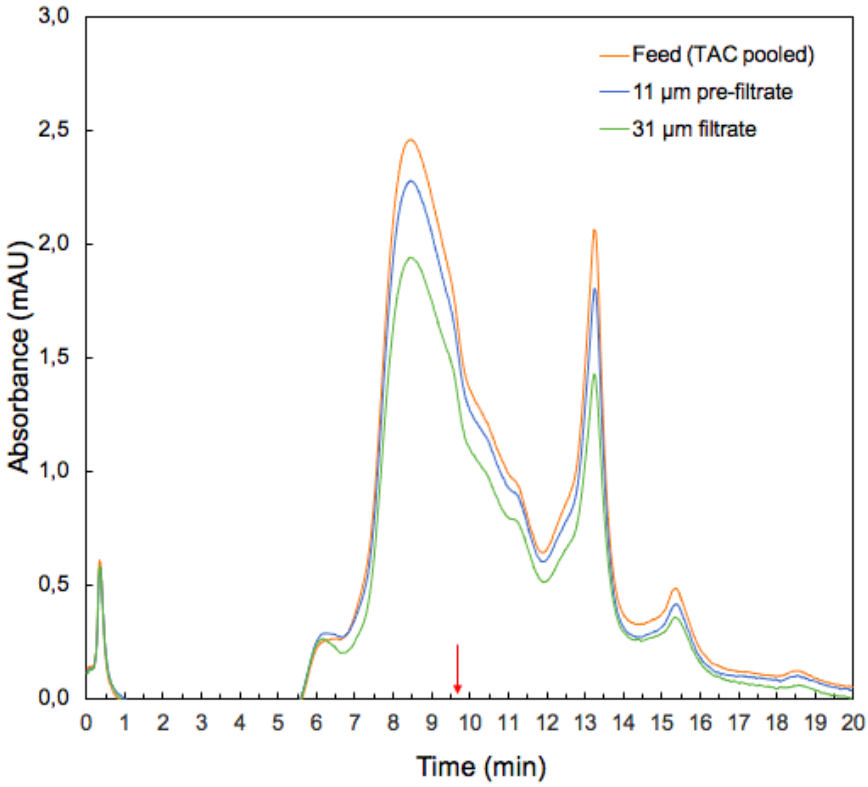

Figure 17. Chromatogram obtained from the SE-HPLC analysis of the feed (TAC pooled), 11 μm pre-filtrate and 33 μm filtrate.

Finally, to qualitatively assess the proteomic composition of the final filtrate, LC-MS/MS was conducted. Table 10 shows the results of LC-MS/MS analysis of the final filtrate. The protein with the highest score and coverage, hence the most likely protein, was identified as "Ig lambda chain C region". The results of the LC-MS/MS analysis suggest that the most abundant species in the filtrate is an Ig-like protein, i.e. most likely IgY. Of the proteins presented in Table 10, serum albumin (α-livetin), IgY (γ-livetin) and vitellogenins are as earlier described, the most abundant proteins in egg yolk. The results from the LC-MS/MS analysis are concordant with the SE-HPLC profile (Fig. 17) on the presence of impurities.

Table 10. Overview of the result from the LC-MS/MS analysis. The result of the analysis is typical for all filtrates (n=3).

UniProt code	Protein identified	Score	Coverage [%]	Mw [kDa]	Isoelectric point [pI]
P20763	Ig lambda chain C region	739.90	90.29	11.4	6.51
A0A3Q2UAA5	Ig-like domain-containing protein	269.09	52.59	12.9	8.03
A0A3Q2U8F2	Ig-like domain-containing protein	193.71	63	10.2	8.97
A0A3Q2TX54	Ig-like domain-containing protein	189.61	65	10.4	8.94
A0A3Q2U343	Ig-like domain-containing protein	189.55	65.35	10.4	7.97
A0A3Q2U474	Ig-like domain-containing protein	161.36	75.25	10.3	9.35
A0A3Q2TX22	Ig-like domain-containing protein	113	55.45	10.4	8.94
A0A1D5P9F9	Uncharacterized protein	103.08	24.30	198.9	7.46
A0A3Q2U5M8	Ig-like domain-containing protein	87.40	60.40	10.3	9.29
F1NFL6	Vitellogenin-2	74.35	6.36	205.0	9.10
F1NK40	Uncharacterized protein	61.37	15.94	163.2	6.37
P10184	Ovoinhibitor	36.57	31.99	51.9	6.58
P19121	Serum albumin	34.17	28.62	69.9	5.74
A0A3Q2U5V5	Ig-like domain-containing protein	31.57	43.62	10.0	5.24
A0A3Q2TZ57	Ig-like domain-containing protein	29.73	46.88	9.9	5.11
A0A3Q2U9M3	Ig-like domain-containing protein	26.25	41.49	9.7	7.96
A0A3Q2U7L8	Ig-like domain-containing protein	24.18	23.96	9.8	5.87
A0A3Q2UG72	Anaphylatoxin-like domain-containing protein	20.82	5.40	176.7	7.81
A0A3Q3AGK3	Ig-like domain-containing protein	19.28	44.44	10.3	4.73
A0A1D5NUW2	Vitellogenin-1	16.72	2.30	210.6	9.0
A0A3Q2U347	Vitellogenin-3	11.57	3.03	186.9	8.84
F1NWX6	Plasminogen	10.88	5.74	90.7	7.65
F1P587	Anaphylatoxin-like domain-containing protein	9.83	2.43	181.0	7.31
O93568	Fibrinogen gamma chain	9.05	8.51	49.6	5.74
A0A3Q2UFU8	Ig-like domain-containing protein	8.14	41.49	9.6	6.44
A0A1D5P3R8	Uncharacterized protein	7.94	2.10	166.2	6.16
Q02020	Fibrinogen beta chain	7.02	5.40	52.6	7.36
F1NI07	Insulin like growth factor binging protein acid labile subunit	6.86	6.96	66.9	7.25
A0A3Q3AX54	Uncharacterized protein	3.61	2.61	134.2	6.99

4.7 Virus removal filtration

Ultimately, a virus removal filtration with "11 μm filtrate" at a load volume of 14.4 L m^{-2} and a concentration of 1 mg ml^{-1} spiked with the ΦX174 phage (28 nm; pI 6.6) was performed in order to assess a LRV for the final preparation of IgY and this method of virus removal. In a typical protein bioprocess, two orthogonal virus clearance steps are implemented in order to ensure the absolute clearance of viral contaminants. For enveloped viruses, a combination of low pH and solvent/detergent treatments is useful for inactivation, but in this processing of IgY, no such step was investigated. The virus removal filtration was conducted with a 31 μm filter at a TMP of 3 bar. The virus titer of the feed was calculated to 6.0±0.6 PFU ml^{-1}.

Table 11 shows the feed titer, filtrate titer as well as the LRV of the virus removal filtration determined with the PFU assay. No plaques were detected. Hence, the filtration exhibited over 5 $\log_{10}$ reduction of the bacteriophage titer as calculated with formula (4).

Table 11. The feed titer, filtrate titer and log reduction value (LRV) for the virus removal filtration of "11 μm filtrate" spiked with ΦX174, measured with the PFU assay. The filtrations were done in triplicate and virus quantification of each sample was done in duplicate.

	Feed titer [$\log_{10}$ PFU ml^{-1}]	Filtrate titer [$\log_{10}$ PFU ml^{-1}]	LRV
Run 1	6.0±0.6	≤0.7	≥5.3±0.6
Run 2	6.0±0.6	≤0.7	≥5.3±0.6

Figure 18a shows the typical result from the PFU assay of the feed solutions (n=3) at three different dilutions (10^{-3}, 10^{-4}, 10^{-5}) (n=2). The virus titres of feed solutions were calculated based on the number of plaques of the 10^{-3} dilutions. Figure 18b shows the filtrate of one filtration without dilutions (10^{0}) (n=2), and the result is typical of all filtrations (n=3).

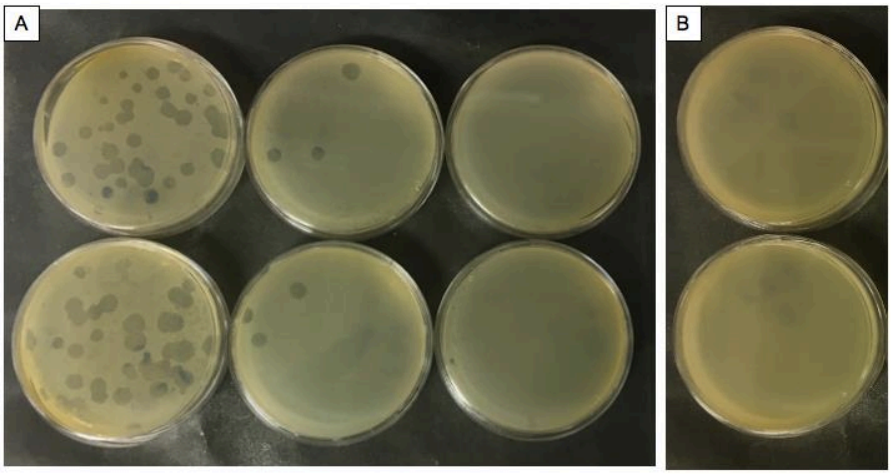

Figure 18. a) From left, top row: Feed 1 with dilutions (from right to left) 10^{-3}, 10^{-4} and 10^{-5}. From left, bottom row: Feed 1 with dilutions (from right to left) 10^{-3}, 10^{-4} and 10^{-5}. b) Filtrate 1 without dilution (100) (n=2). The results are typical for the feeds and filtrates from all filtrations (n=3).

5 Main conclusions

The main aim of this thesis was to study the feasibility of IgY nanofiltration with mille-feuille filter paper. In order to do so, IgY first had to be isolated and purified from chicken egg yolk, using crude isolation and polishing chromatography. In a real protein purification process, additional purification steps would be implemented in order to generate a high purity of the final product, e.g. with a second polishing chromatography step and adsorptive depth filters to clear the feed from protein aggregates and cell harvest. When a nanofiltration is conducted for viral clearance in the final step of the downstream process, the feed has ideally a high purity which contributes to an enhanced throughput and thus to a higher biosafety and recovery of the final product.

SDS-PAGE analysis of the crude isolation product, generated after PEG precipitation, resembled those that have been reported earlier, i.e. with protein bands at 65 and 25-30 kDa, representing IgY-HC and IgY-LC respectively, as well as a number of bands seen at 75, 40, 35 and 10 kDa. In terms of yield after PEG precipitation, the estimated recovery amounted to 52-63 mg of IgY per yolk (15 ml) which is within the range of those earlier mentioned in other studies, i.e. between 40 and 132 mg per yolk (15 ml). The IEX chromatography displayed column overload and was therefore not further used. TA chromatography generated a yield of 65-75% and was further used in the purification of IgY for the virus removal filtration. Two-step filtration was implemented to process the TAC-pooled product, for which two types of filters were produced, i.e. 11 μm pre-filter and 31 μm dedicated virus removal filter. The pre-filter featured larger pores than 31 μm virus filter and higher hydraulic flux. The pre-filters efficiently removed any large molecular weight species and protein aggregates present in the TAC-pooled preparation, which was manifested by rapid fouling during pre-filtration. During the subsequent filtration through 31 μm virus filters the flux decay was negligible. It was further observed that filtration through 31 μm virus filters resulted in further removal of large molecular weight impurities. Hence, it was clear that the two-step filtration approach had critical impact on the quality of the final product. Proteomic analysis with SE-HPLC and LC-MS/MS confirmed that IgY was indeed the main constituent of the final filtrate (31 μm filtrate), although various other impurities were detectable too. To reach a higher purity of IgY, additional polishing chromatography steps, e.g. ion exchange chromatography already tested or preparative scale gel chromatography, adsorptive depth filtration or a combination of both should be implemented.

Ultimately, the final IgY preparation was spiked with 28 nm ΦX174 phage to study the virus clearance efficiency. The resulting LRV amounted to >5, demonstrating that the mille-feuille filter paper could provide high level of biosafety for heat-sensitive protein-based nutraceuticals. Additional inactivation steps could be desirable to implement, e.g. low pH and solvent/detergent treatments in order to inactivate enveloped viruses. The results from this thesis will be significant in the further research of the mille-feuille filter paper and its establishment on the market as a high-performing cost-efficient nanofilter in the viral clearance of protein-based nutraceuticals.

6 Acknowledgements

First, I would like to thank my supervisor, professor Albert Mihranyan, for creating this master thesis project and for his support throughout the project. I also want to thank Levon Manukyan, Marilena Marinaki and Thanos Mantas for their help in my laboratory work, but also for their kindness and overall support. I also want to thank my subject reader professor Gunnar Johansson for his feedback on this thesis. Finally, many thanks to my family for their endless love and support.

7 References

Al-Razem, F., Amro, W.A., Al-Qaisi, W. 2018, “Production and purification of IgY antibodies from chicken egg yolk”, Journal of Genetic Engineering and Biotechnology, vol. 16, no. 1, pp. 99-103.

Akita, E.M., Nakai, S. 1993, “Comparison of four purification methods for the production of immunoglobulins from egg laid by hens immunized with an enterotoxigenic E.coli strain”, *Journal of Immunological Methods*, vol.160, no. 2, pp. 207-214.

Asper, M., Hanrieder, T., Quellmalz, A., Mihranyan, A. 2015, “Removal of xenotropic murine leukemia virus by nanocellulose based filter paper”, Biologicals, vol. 43, no. 6, pp. 452-456.

Barrett, E.P. & Joyner, L.G. 1951, “Determination of Nitrogen Adsorption-Desorption Isotherms” *Analytical Chemistry*, vol. 23, no. 5, pp. 791-792.

Boschetti, N., Stucki, M., Späth, P.J., Kempf, C. 2005, "Virus safety of intravenous immunoglobulin: Future challenges", *Clinical Reviews in Allergy & Immunology,* vol. 29, no. 3, pp. 333-344.

Buchacher, A. & Iberer, G. 2006, "Purification of intravenous immunoglobulin G from human plasma – aspects of yield and virus safety", *Biotechnology Journal,* vol. 1, no. 2, pp. 148-163.

Carlander, D., Stålberg, J., Larsson, A. 1999, “Chicken Antibodies”, *Upsala Journal of Medical Sciences*, vol. 104, no. 3, pp. 179-189.

Carlander, D., Kollberg, H., Wejåker, P., Larsson, A. 2000, "Peroral immunotheraphy with yolk antibodies for the prevention and treatment of enteric infections", *Immunologic Research,* vol. 21, no. 1, pp. 1-6.

Cipriano, D., Burnham, M., Hughes, J.V. 2012, "Effectiveness of various processing steps for viral clearance of therapeutic proteins: Database analyses of commonly used steps", *Methods in Molecular Biology*, vol. 899, no.1, pp. 277.

Deignan, T., Kelly, J., Alwan, A., O'Farrelly, C. 2000, "Comparative Analysis of Methods of Purification of Egg Yolk Immunoglobulin", *Food and Agricultural Immunology,* vol. 12, no. 1, pp. 77-85.

Godden, S., McMartin, S., Feirtag, J., Stabel, J., Bey, R., Goyal, S., Metzger, L., Fetrow, J., Wells, S., Chester-Jones, H. 2006, "Heat-Treatment of Bovine Colostrum. II: Effects of Heating Duration on Pathogen Viability and Immunoglobulin G", *Journal of Dairy Science,* vol. 89, no. 9, pp. 3476-3483.

Grieb, T., Forng, R., Brown, R., Owolabi, T., Maddox, E., Mcbain, A., Drohan, W.N., Mann, D.M., Burgess, W.H. 2002, "Effective use of Gamma Irradiation for Pathogen Inactivation of Monoclonal Antibody Preparations", *Biologicals,* vol. 30, no. 3, pp. 207-21

Gröner, A., Broumis, C., Fang, R., Nowak, T., Popp, B., Schäfer, W., Roth, N.J. 2018, "Effective inactivation of a wide range of viruses by pasteurization", *Transfusion,* vol. 58, no. 1, pp. 41-51.)

Gustafsson, S., Lordat, P., Hanrieder, T., Asper, M., Schaefer, O., Mihranyan, A., 2016, "Mille-feuille paper: a novel type of filter architecture for advanced virus separation applications", *Materials Horizons,* vol. 3, no. 4, pp. 320-327.

Gustafsson, S. & Mihranyan, A. 2016, "Strategies for tailoring the pore-size distribution of virus retention filter papers", *ACS Applied Materials and Interfaces*, vol. 8, no.22, pp. 13759-13767.

Gustafsson, O., Manukyan, L., Mihranyan, A. 2018, "High Performance Virus Removal Filter Paper for Drinking Water Purification", *Global Challenges*, vol. 2, no. 1800031, pp. 29-36.

Hansen, P., Scoble, J.A., Hanson, B., Hoogenraad, N.J. 1997, "Isolation and purification of immunoglobulins from chicken eggs using thiophilic interaction chromatography", *Journal of Immunological Methods*, vol. 210, pp. 1-7.

Hernández-Campos, F.J., Brito-De la Fuente, E., Torrestiana-Sánchez, B. 2010, "Purification of Egg Yolk Immunoglobulin (IgY) by Ultrafiltration: Effect of pH, Ionic Strength, and Membrane Properties", *Journal of Agricultural and Food Chemistry,* vol. 58, no. 1, pp. 187-193.

Horie, K., Horie, N., Abdou, A.M., Yang, J.-., Yun, S.-., Chun, H.-., Park, C.-., Kim, M., Hatta, H. 2004, "Suppressive Effect of Functional Drinking Yogurt Containing Specific Egg Yolk Immunoglobulin on Helicobacter pylori in Humans", *Journal of Dairy Science,* vol. 87, no. 12, pp. 4073-4079.

Hutchens, T.W. & Porath, J. 1986, "Thiophilic adsorption of immunoglobulins—Analysis of conditions optimal for selective immobilization and purification", *Analytical Biochemistry,* vol. 159, no. 1, pp. 217-226.

Jensenius, J., Andersen, I., Hau, J., Crone, M., Koch, C. 1981, "Eggs: conveniently packed antibodies. Methods for purification of yolk IgG", *Journal of Immunological Methods*, vol. 46, pp. 63-68.

Jin, W., Jin, W., Xing, Z., Song, Y., Song, Y., Huang, C., Huang, C., Xu, X., Xu, X., Ghose, S., Li, Z.J., Li, Z.J. 2019, "Protein aggregation and mitigation strategy in low pH viral

inactivation for monoclonal antibody purification", *mAbs,* vol. 11, no. 8, pp. 1479-1491.

Jones, D.R., Anderson, K.E., Guard, J.Y. 2012, "Prevalence of coliforms, Salmonella, Listeria, and Campylobacter associated with eggs and the environment of conventional cage and free-range egg production", *Poultry Science,* vol. 91, no. 5, pp. 1195-1202.

Kent, J.A., Bommaraju, T.V., Barnicki, S.D., SpringerLink (Online service) 2017, *Handbook of Industrial Chemistry and Biotechnology,* , Springer International Publishing, Cham., vol. 13, pp. 1663.

Kim, W.K. & Patterson, P.H. 2003, "Production of an egg yolk antibody specific to microbial uricase and its inhibitory effects on uricase activity", *Poultry Science,* vol. 82, no. 10, pp. 1554-1558.

Landry, M.R. 2005, "Thermoporometry by differential scanning calorimetry: experimental considerations and applications", *Thermochimica Acta,* vol. 433, no. 1, pp. 27-50.

Larsson, A., Carlander, D., Wilhelmsson, M. 1998, "Antibody response in laying hens with small amounts of antigen", *Food and Agricultural Immunology,* vol. 10, no. 1,

Lathe, G.H. & Ruthven, C.R.J. 1956, "The separation of substances and estimation of their relative molecular sizes by the use of columns of starch in water", *Biochemical Journal,* vol. 62, no. 4, pp. 665-674.

Leslie, G.A. & Clem, L.W. 1969, "Phylogen of immunoglobulin structure and function. 3. Immunoglobulins of the chicken", *The Journal of experimental medicine,* vol. 130, no. 6, pp. 1337.

Li, G., Stewart, R., Conlan, B., Gilbert, A., Roeth, P., Nair, H. 2002, "Purification of human immunoglobulin G: a new approach to plasma fractionation", *Vox Sanguinis,* vol. 83, no. 4, pp. 332-338.

Mann, K. & Mann, M. 2008, "The chicken egg yolk plasma and granule proteomes", *PROTEOMICS,* vol. 8, no. 1, pp. 178-191.

Manukyan, L., Mantas, A., Razumikhin, M., Katalevsky, A., Golubev, E., Mihranyan, A. 2020, "Two-Step Size-Exclusion Nanofiltration of Prothrombin Complex Concentrate Using Nanocellulose-Based Filter Paper", *Biomedicines,* vol. 8, no. 4, pp. 69.

Manukyan, L., Gustafsson, O., Gustafsson, S., Tummala, G.K., Begum, A., Alfasane, M.A., Siddique-e-Rabbani, K., Mihranyan, A. (2019), “Scaleable and Sustainable Total Pathogen Removal Filter Paper for Point-of-Use Drinking Water Purification in Bangladesh”, *ACS Sustainable Chemistry and Engineering*, vol. 7, no. 17, pp. 14373-14383.

Marques, B.F., Roush, D.J., Göklen, K.E. 2009, “Virus filtration of high-concentration

monoclonal antibody solutions", *Biotechnology Progress*, vol. 25, no. 2, pp. 483-491.

Metreveli, G., Wågberg, L., Emmoth, E., Belak, S., Strømme, M., Mihranyan, A. 2014, "Size-exclusion nanocellulose filter paper for virus removal", *Advanced Healthcare Materials*, vol. 3, no. 10, pp. 1546-1550.

Mine, Y. & Kovacs-Nolan, J. 2006, "New insights in biologically active proteins and peptides derived from hen egg", *World's Poultry Science Journal,* vol. 62, no. 1, pp. 87-96.

Pappin, D.J.C., Hojrup, P., Bleasby, A.J. 1993, "Rapid identification of proteins by peptide-mass fingerprinting", *Current Biology,* vol. 3, no. 6, pp. 327-332.

Pauly, D., Chacana, P.A., Calzado, E.G., Brembs, B., Schade, R. 2011, "IgY technology: extraction of chicken antibodies from egg yolk by polyethylene glycol (PEG) precipitation", *Journal of visualized experiments,* no. 51, pp. 3084.

Polson, A., Coetzer, T., Kruger, J., von Maltzahn, E., van der Merwe, K. J. 1985, "Improvements in the isolation of igY from the yolks of eggs laid by immunized hens", *Immunological Investigations,* vol. 14, no. 4, pp. 323-327.

Polson, A., von Wechmar, Barbara., van Regenmortel, M.H.V. 1980, "Isolation of viral IgY antibodies from yolks of immunized hens", *Immunological Communications,* vol. 9**,** pp. 475-493.

Porath, J., Belew, M. 1987, "'Thiophilic' interaction and selective adsorption of proteins", *Trends in Biotechnology*, vol. 5, no. 8, pp. 225-229.

Reed L, Muench H. 1938, "A simple method of estimating fifty percent endpoints" *American Journal of Hygiene,* vol. 27, no. 493, pp.7.

Sahin, Z., Demir, Y.K., Kayser, V. 2016, "Global kinetic analysis of seeded BSA aggregation", *European Journal of Pharmaceutical Sciences,* vol. 86, pp. 115-124.

Sapan, C.V., Lundblad, R.L., Price, N.C. 1999, "Colorimetric protein assay techniques", *Biotechnology and Applied Biochemistry,* vol. 29, no. 2, pp. 99-108.

Sarker, S.A., Casswall, T.H., Juneja, L.R., Hoq, E., Hossain, I., Fuchs, G.J., Hammarström, L. 2001, "Randomized, Placebo-Controlled, Clinical Trial of Hyperimmunized Chicken Egg Yolk Immunoglobulin in Children With Rotavirus Diarrhea", *Journal of Pediatric Gastroenterology and Nutrition,* vol. 32, no. 1, pp. 19-25.

Schade, R., Nehn, I., Erhard, M., Hlinak, A., Staak, C. 2001, *"Chicken Egg Yolk Antibodies, Production and Application" Springer- Verlag*, pp. 65–107.

Scopes R K. 1994. “Separation by Adsorption II: Ion Exchangers and Nonspecific adsorbents”, *Protein Purification: Principles and Practice*, vol. 3, pp 146- 185.

Shapiro, A.L., Viñuela, E. & V. Maizel, J. 1967, "Molecular weight estimation of polypeptide chains by electrophoresis in SDS-polyacrylamide gels", *Biochemical and Biophysical Research Communications,* vol. 28, no. 5, pp. 815-820.

Shiba, K., Niidome, T., Katoh, E., Xiang, H., Han, L., Mori, T., Katayama, Y. 2010, "Polydispersity as a Parameter for Indicating the Thermal Stability of Proteins by Dynamic Light Scattering", *Analytical Sciences,* vol. 26, no. 6, pp. 659-663.

Shukla, A.A., H. Aranha. 2015, “Viral clearance for biopharmaceutical downstream processes”, Pharmaceutical Bioprocessing, vol. 3, no. 2, pp. 127-138.

Wu, L., Manukyan, L., Mantas, A. Mihranyan, A. 2019, ”Filter Paper for Virus Removal Filtration of Human Intravenous Immunoglobulin”, *ACS Applied Nano Materials*, vol. 2, no. 10, pp. 6352-6359

Yolken, R.H., Leister, F., Wee, S.B., Miskuff, R., Vonderfecht, S. 1988, "Antibodies to rotaviruses in chickens' eggs: a potential source of antiviral immunoglobulins suitable for human consumption", *Pediatrics,* vol. 81, no. 2, pp. 291.